NATIONAL ADVISORY COMMITTEE FOR AERONAUTICS

TECHNICAL NOTE

No. 1283

THE LANGLEY TWO-DIMENSIONAL LOW-TURBULENCE PRESSURE TUNNEL

By Albert E. von Doenhoff and Frank T. Abbott, Jr.

Langley Memorial Aeronautical Laboratory
Langley Field, Va.

Washington
May 1947

NATIONAL ADVISORY COMMITTEE FOR AERONAUTICS

TECHNICAL NOTE NO. 1283

THE LANGLEY TWO-DIMENSIONAL LOW-TURBULENCE PRESSURE TUNNEL

By Albert E. von Doenhoff and Frank T. Abbott, Jr.

SUMMARY

A description is presented of the Langley two-dimensional low-turbulence pressure tunnel and a history is given of the work done at the Langley Memorial Aeronautical Laboratory which led to the achievement of a remarkably low level of turbulence in the air stream of this wind tunnel. The types of investigations to which the tunnel is suited and the methods of obtaining and correcting data are also discussed.

INTRODUCTION

Prior to the construction of the Langley two-dimensional low-turbulence pressure tunnel, the largest amount of comparable airfoil data was obtained from tests in the NACA variable-density tunnel at a test Reynolds number of approximately 3×10^6. The turbulence level of the NACA variable-density tunnel was quite high as indicated by the low value of critical Reynolds number for a sphere (150,000). Although the effective Reynolds number concept appeared to be valid for some types of airfoil sections with regard to maximum lift, it did not appear to give satisfactory corrections for drag coefficients measured in a turbulent air stream. (See reference 1.)

An investigation of tapered wings by Anderson (reference 2) indicated that the characteristics of wings of usual plan form could be satisfactorily computed from the aerodynamic characteristics of the component airfoil sections. It seemed desirable, therefore, to design a tunnel especially for testing airfoil sections and capable of obtaining data at Reynolds numbers at least as high as would be reached by any airplane likely to be designed in the near future. Such considerations led to the design and construction of the Langley two-dimensional low-turbulence pressure tunnel.

Characteristics particularly desired for this tunnel were full-scale Reynolds numbers, extremely low air-stream turbulence, and convenient model size. Full-scale Reynolds numbers are obtained with moderate amounts of power by compressing the air in the wind tunnel to increase its density and by mounting models so that the test section is completely spanned. Increasing the density of the air to 10 times its normal value gives a corresponding increase in Reynolds number since there is essentially no change in absolute viscosity due to change in pressure in this range of pressures. Mounting models so that the test section is completely spanned allows the Reynolds number to be increased by making possible a much larger ratio of model size to tunnel cross section since the air flow acts only in two dimensions and cross flows around the ends of the span are prevented. Mounting the models in this manner is also advantageous in tests of section characteristics since the difficulties associated with aspect ratio and tare corrections are eliminated.

Low turbulence was made possible by using a large area reduction between the entrance cone and the test section and by the introduction of a number of fine-wire small mesh screens in the entrance cone.

The sizes of the models, varying from approximately 24 inches to 100 inches, are small enough to permit them to be easily handled without the aid of auxiliary hoists, yet large enough that maintaining adequate model accuracy is not too difficult.

Acknowledgement is gratefully expressed for the expert guidance and many original contributions of Mr. Eastman N. Jacobs, who supervised the design of the tunnel and the development of many of the experimental techniques.

SYMBOLS

A	area of individual integrating manometer tube
a	airfoil mean line designation, fraction of chord from leading edge over which design load is uniform; also in derivation of equation for integrating manometer, height of liquid in manometer when same pressure is applied to all tubes
B	dimensionless constant determining width of wake

b in derivation of integrating manometer equation, height of liquid in integrating tube when pressure distribution is applied to manometer and reference pressure is applied to integrating tube and reference tubes

c chord

c_d section drag coefficient

c_d' section drag coefficient uncorrected for tunnel-wall effects

c_{d_T} section drag coefficient measured in tunnel

c_l section lift coefficient

c_l' section lift coefficient uncorrected for tunnel-wall effects

c_{l_T} section lift coefficient measured in tunnel

c_{l_i} design section lift coefficient

$c_{m_{c/4}}$ moment coefficient about quarter-chord point

$c_{m_{c/4}}'$ moment coefficient about quarter-chord point measured in tunnel

F average of velocity readings of orifices on floor and ceiling used to measure blocking at high lifts

F_o average value of F in low-lift range

f_{SP} calibration factor for measured tunnel static pressure

H_o free-stream total pressure

H_w total pressure in wake

H_c coefficient of loss of total pressure in wake $\left(\frac{H_o - H_w}{q_o}\right)$

h_T tunnel height

$h_{1,2,\ldots i}$ height of liquid in any individual tube when pressure distribution is applied to manometer

$K = \frac{c_d'}{c_{d_T}}$

k	in derivation of integrating manometer equation, ratio of combined area of tubes connected to reference pressure to area of a tube connected to an individual orifice
L	length over which pressure measurements are made
ΔL	distance between uniformly spaced pressure orifices
M	Mach number
n	number of individual tubes in integrating manometer or individual pressure orifices
P_R	resultant pressure coefficient, difference between local upper-surface and lower-surface pressure coefficients
p	local pressure on airfoil surface
p_L	static pressure at any point on tunnel floor within length L
p_U	static pressure at any point on tunnel ceiling within length L
p_w	static pressure in wake
$p_{1,2,\ldots i}$	pressure applied to individual manometer tube
p_r	reference pressure
q	free-stream dynamic pressure at position of turbulence-reducing screens
q_o	free-stream dynamic pressure in test section
q_o'	free-stream dynamic pressure in test section uncorrected for tunnel wall effects
R	Reynolds number $\left(\frac{Vc}{\nu}\right)$
R_δ	boundary-layer Reynolds number $\left(\frac{V\delta}{\nu}\right)$
s	pressure coefficient $\left(\frac{H_o - p}{q_o}\right)$
S_w	static-pressure coefficient in wake $\left(\frac{H_o - p_w}{q_o}\right)$

V free-stream velocity

ΔV increment in free-stream velocity due to blocking

V' corrected indicated tunnel velocity

V'' tunnel velocity measured by static-pressure orifices

v velocity at any point on surface of airfoil

x distance along airfoil chord or center line of tunnel

Y variable of integration $\left(\frac{By_W}{c}\right)$

y distance perpendicular to stream direction

Δy spacing of total-pressure tubes in rake

y_t ordinate of symmetrical thickness distribution

y_W distance perpendicular to stream direction from position of $H_{c_{max}}$

$\frac{dy_t}{dx}$ slope of surface of symmetrical thickness distribution

α_{l_o} angle of zero lift

α_o section angle of attack corrected for tunnel-wall effects

α_o' section angle of attack measured in tunnel

Δp_{SP} difference in manometer readings used to measure tunnel dynamic pressure $(q_o' = \Delta p_{SP} \rho f_{SP})$

δ distance normal to a surface from surface to point in boundary layer where dynamic pressure is one-half its local value outside boundary layer

η ratio of measured lift to actual lift for any type of lift distribution

η_a η-factor for additional-type loading

η_b η-factor for basic mean-line loading

η_x η-factor applying to a point vortex

Λ component of blocking factor dependent on shape of body

ν kinematic viscosity

ξ quantity used for correcting effect of body upon velocity measured by static-pressure orifices

ρ density of manometer liquid

σ component of blocking factor dependent on size of body

HISTORY OF DEVELOPMENT

Description of the Langley Two-Dimensional Low-Turbulence Tunnel

Because the shape of the air passages of the proposed pressure tunnel were unusual, and because of the fact that the means proposed for obtaining low turbulence had never been checked at high Reynolds numbers, it was desirable to build a model of the proposed tunnel to study its flow characteristics and to develop means for producing a satisfactory air stream. The Reynolds number of tests in such a model tunnel had to be at least as high as those in the lower range of flight Reynolds numbers in order to obtain a reliable indication of the effective turbulence level. A full-size model of the proposed tunnel, designed to operate only at atmospheric pressure, was therefore built. This tunnel is called the Langley two-dimensional low-turbulence tunnel.

This tunnel was completed in April 1938. It was originally designated the NACA ice tunnel because of the incorporation of refrigerating equipment in the design to permit icing experiments. The tunnel is of closed throat type, built of wood with a sheet steel lining. Because of the contemplated icing experiments, it was heavily insulated on the outside. Figure 1 shows the shape of the air passages of this tunnel. The test section is rectangular in shape, $7\frac{1}{2}$ feet high, and 3 feet wide, and was designed so that models could be tested completely spanning the 3-foot width. The test section is $7\frac{1}{2}$ feet long but models having chords as large as 100 inches have been tested. Power supplied by a 200-horsepower direct-current motor provides a maximum speed of about 155 miles per hour with a dynamic pressure of about 60 pounds per square foot. These conditions give a maximum Reynolds number of about 1.4×10^6 per foot of model chord.

Surveys of the air stream of the test section showed a variation in static and dynamic pressure of less than 0.25 percent of the dynamic pressure in the region normally occupied by the model. The angular variation of the air-stream direction in the same region was less than 0.2°. The variation in static pressure longitudinally over the length of the test section was 0.5 percent with a variation of only 0.25 percent over a 2-foot length at the model mounting point. Uniformity of the pressure gradient in a longitudinal direction was obtained by adjusting slots in the vertical walls of the test section to allow air to bleed out. A positive pressure is built up in the test section to accomplish this bleeding by means of a blower which discharges air into the tunnel through an annular slot downstream of the test section.

Boundary-layer control of the short exit cone of this tunnel, an unusual feature, is accomplished by means of two annular slots as shown in figure 1. Air from the boundary layer of the exit cone is sucked into the upstream slot by means of a 45-horsepower blower and is discharged into the tunnel with increased velocity through the downstream slot.

Previous experience with the Langley smoke-flow tunnel indicated that turbulence could be reduced by the use of a large area reduction through the entrance cone and dense screens in the large section ahead of the entrance cone. This experience was used in the design of the Langley two-dimensional low-turbulence tunnel. The section of the tunnel immediately ahead of the entrance cone was made 21 feet square, which gives an area reduction of about 19.6 to 1 between this section and the test section. In this large section a honeycomb made with 9-inch-square cells was installed. On the upstream side, the honeycomb was covered with a 30-mesh standard wire screen, and on the downstream side with a 60-mesh screen made of 0.0065-inch-diameter wire. The honeycomb was made up of nine sections, each 7 feet square. The unusually rapid expansion of the tunnel air passage immediately upstream of the honeycomb screens considerably reduced the length of the air passage. Such a rapid expansion is permissible because the dynamic pressure of the air stream at this point is relatively low and any unevenness of flow is smoothed out by the high pressure drop of the honeycomb screens.

The first airfoil tests were made on a low-drag type of airfoil section, and the measured drag coefficient was 0.0030, about 50 percent less than had previously been measured on an airfoil of comparable thickness. This test was carried out in June 1938. Comparison of this drag coefficient with the laminar and turbulent skin-friction curves showed that the flow over the airfoil was laminar over more than half the surface. Comparison

of other airfoil test results with those obtained in flight also indicated that a very low turbulence level had been achieved. It was not considered probable, however, that the desired effective zero turbulence level, that is, a level at which the air-stream turbulence would have a vanishing effect upon boundary-layer transition, had been reached. Under favorable conditions, boundary-layer Reynolds numbers, R_δ, of about 5000 were measured in the tunnel for some airfoils compared with R_δ of 7500 to 9000 obtained in flight. (See reference 3.)

Turbulence measurements made in January 1940 with a National Bureau of Standards hot-wire anemometer also indicated that the air stream had a reasonably low turbulence level compared with other wind tunnels. The horizontal turbulence components, which are of the same order of magnitude as the vertical and longitudinal components, are plotted against Reynolds number in figure 2 and against spanwise position in figure 3. The spanwise survey indicated that large variations in the turbulence level were present at points corresponding to the relative positions of the joints between the 7-foot sections of the honeycomb upstream.

Turbulence measurements obtained by comparison of the critical Reynolds numbers of spheres were not made in the Langley two-dimensional low-turbulence tunnel. Previous comparative tests of spheres in the Langley 8-foot high-speed tunnel (reference 4) and in free air (reference 5) gave about the same results. Since tests of the NACA 0012 airfoil in the Langley 8-foot high-speed tunnel (reference 6) and in the Langley two-dimensional low-turbulence tunnel (reference 7) indicated a lower turbulence level in the latter tunnel, it was concluded that the general level of turbulence was too low for the sphere tests to give significant results.

Investigation to Reduce Turbulence Level

The results of turbulence surveys and comparative tests in the Langley two-dimensional low-turbulence tunnel and in flight clearly showed the desirability of further reduction of the turbulence level of the tunnel. The turbulence surveys also showed the necessity of eliminating, insofar as possible, the effects of any joints and supports of the screen. This result was believed to be obtainable by the proper installation of a number of additional screens.

Preliminary consideration of the physical factors involved suggested the likelihood that for a given pressure drop a number

of screens placed one behind the other would be more effective in reducing the turbulence level than a single screen to produce the given pressure drop. (This reasoning was later substantiated by a more detailed investigation by Dryden and his collaborators who were also working on the problem of turbulence reduction at about the same time at the National Bureau of Standards.) The realization that some defects might be present in any screen installation led to the suggestion that a number of screens, each with a pressure drop of about one q, would be a good compromise (where q is the dynamic pressure of the air stream at the screens). In a screen installation with such a pressure drop, the effects of the wake of a plugged spot would be expected to be about the same as the effects of the jet of an open spot.

Experiments were conducted during the latter part of 1939 in the Langley smoke-flow tunnel to obtain data that might be used in the design of an improved screen installation for the Langley two-dimensional low-turbulence tunnel. Screen models were mounted in the test section of the smoke-flow tunnel and visual observations were made of the smoke flow through the screen. Screens having a pressure drop of the order of one q were observed to have a marked effect on breaking up large eddies and to reduce markedly the magnitude of the fluctuating velocities associated with each eddy. With a 2-mesh screen having a wire diameter of 0.1 inch, it was found that, when the speed exceeded approximately 3 feet per second, the nature of the flow through the screen changed. Although the turbulence associated with large eddies was broken up, small-scale eddies were introduced by the wires themselves. Below this critical speed the flow appeared to be of the viscous type and no small eddies were observed.

On the basis of these experiments, consideration was given to the size of wire for the screens that were to be installed in the Langley two-dimensional low-turbulence tunnel in order that the Reynolds number for viscous flow might not be exceeded at the highest tunnel speed and thus turbulence from the wires themselves might be avoided. A wire size of 0.0065 was found to be suitable and, in order to obtain the desired pressure drop of one q, a 30-mesh screen with this wire diameter was selected.

Information published by Taylor on the decay of turbulence behind screens (reference 8) indicated that a spacing between the screens of approximately 100 times the length of one screen mesh would be more effective than closer spacing, so that, if turbulence were produced by any screen, this turbulence would have a chance to die out before reaching the next screen. The number of screens needed was indefinite, and the final level of

turbulence seemed to be determined by the amount of turbulence introduced by the last screen. Great care was therefore believed necessary in the fabrication and installation of the screens.

The screen wire was made of phosphor bronze and was woven in strips 7 feet wide with a special selvage as shown in figure 4(a). Three strips were sewed together with 0.0065-inch diameter wire, the strand of wire through each mesh at the selvage being carefully looped in such a manner that there was no overlapping of the strips and a joint was produced which presented minimum discontinuity. Brass strips were fastened around the four sides of the completed screen panel and the assembly was hung in place in the tunnel on springs, spaced 1 foot apart, attached to the brass-edge strips through cables and turnbuckles. Enough tension was put in the springs to hold the screen taut but not to allow the stress produced in the wires of the screen by the air stream and by tunnel expansion to be too high. Seven layers of screens, spaced 3 inches, were installed in the large section of the tunnel downstream of the honeycomb. Figure 4(b) shows schematically a section of one edge of the screen and the baffles which direct the air stream through the screens. The installation was completed in October 1940.

Turbulence measurements were again made with the National Bureau of Standards hot-wire apparatus in January 1941. The results, as shown in figures 2 and 3, indicated that the level of turbulence had been reduced to the order of one-tenth that of the turbulence level before the screen installation (to about 0.01 to 0.02 percent of free-stream velocity). The large spanwise variation formerly caused by the joints in the honeycomb was now seen to be very small. A gradual rise in the turbulence level with increased tunnel speed was found. This gradual rise in turbulence level might be influenced by an increase in noise level with increase in propeller speed. It may be pointed out that the turbulence level measured was so low that it approached the limit of accuracy of the apparatus.

Figure 5 shows the results of drag surveys on the NACA 67-215 airfoil section before and after the installation of the turbulence-reducing screens. The Reynolds number at which the drag began to rise with increasing Reynolds number showed a marked increase after the screens were installed. Since model conditions were the same for both tests, this increase indicates that the reduction in turbulence level was sufficient to affect the drag appreciably.

Information and experience obtained from work on the Langley two-dimensional low-turbulence tunnel proved invaluable

in the design and operation of the Langley two-dimensional low-turbulence pressure tunnel and was undoubtedly a large factor in the success of the latter tunnel.

THE LANGLEY TWO-DIMENSIONAL LOW-TURBULENCE PRESSURE TUNNEL

Description

Size and range of pressures.- The Langley two-dimensional low-turbulence pressure tunnel is a single-return closed-throat tunnel, the general arrangement of which is shown in figures 6 and 7. The tunnel is constructed of heavy steel plate so that the pressure of the air may be varied from approximately full vacuum to 10 atmospheres absolute, thereby giving a wide range of air densities. Reciprocating compressors with a capacity of 1200 cubic feet of free air per minute provide compressed air. Since the tunnel shell has a volume of about 83,000 cubic feet, a compression rate of approximately one atmosphere per hour is obtained. The tunnel has not been operated at pressures less than atmospheric.

The test section is rectangular in shape, 3 feet wide, $7\frac{1}{2}$ feet high, and $7\frac{1}{2}$ feet long. Figure 8 is a view of the test section looking downstream. The air stream enters the test section through a relatively short entrance cone from a large square section giving a contraction ratio of 17.6 to 1.

The over-all size of the wind-tunnel shell is about 146 feet long and 58 feet wide with a maximum diameter of 26 feet. The test section and entrance and exit cones are surrounded by a 22-foot diameter section of the shell to provide a space to house much of the essential equipment. This space is called the test chamber. Figure 9 shows a view of the interior of the test chamber.

Curved turns at the ends of this tunnel are used instead of the conventional right angle corners to minimize the stress concentrations associated with the high air pressures used. The use of continuous splitter vanes instead of guide vanes, in the large turn as shown in figure 7(b), was also for structural reasons rather than aerodynamic.

An air lock is provided to allow access to the test chamber and test section when the tunnel is at pressures other than atmospheric. Use of the air lock by operating personnel is limited to pressures of not over 4 atmospheres absolute.

The wind tunnel is anchored at one centrally located point and is supported at other points by flexible columns and sliding shoes in order to allow for movement due to temperature and pressure stresses.

Previous experience in the Langley smoke-flow tunnel had indicated that convective currents caused by unequal heating of various parts of the air stream could introduce appreciable amounts of turbulence. A sun shade was therefore provided over the top of the tunnel shell to reduce the differences in temperature between the upper and lower parts of the air stream due to solar heating of the upper part of the shell.

Drive and control system.- The air stream of the Langley two-dimensional low-turbulence pressure tunnel is driven by a 20-blade aluminum-alloy propeller having a diameter of 13 feet. Countervanes directly downstream of the propeller are provided to remove the twist from the air stream. The pitch of the propeller blades and the angle of the countervanes are adjustable, but no change in setting is necessary for the present operating range because the motor develops approximately full power over a 2 to 1 speed range. The propeller hub is enclosed by a 5-foot-diameter fairing. The propeller shaft extends through a packing gland in the tunnel shell and is connected to the motor located in an adjoining building.

The drive motor is a 2000-horsepower separately excited direct-current motor. Power is supplied to the drive motor from a motor generator set. The field circuits of both the motor and the generator are equipped with vacuum-tube voltage regulators to minimize fluctuations in speed. Speed can be easily controlled throughout the entire range from idling speed to 600 rpm by varying the generator voltage and the motor field by manual movement of rheostats in the regulator-control circuit.

Tunnel speed is measured on a manometer in terms of the uncorrected dynamic pressure q_o' of the air stream in the test section. An indication of the value of q_o' is obtained from the difference between the pressures on an impact (total pressure) tube located in the large section of the tunnel ahead of the entrance cone and the static pressure on static orifices located a short distance upstream of the test section. Both the total-pressure tube and the static-pressure orifices were calibrated

against a standardized wind-tunnel calibrating pitot-static tube mounted in the tunnel test section. Factors with which to correct the measured total pressure and static pressures were thus obtained. The dynamic-pressure, Reynolds number, and Mach number range of the tunnel for various tank pressures are shown in figure 10.

Screen installation.- A screen installation patterned after the previously described screen installation in the Langley two-dimensional low-turbulence tunnel was made in the new pressure tunnel. (See fig. 11.) Eleven screens were installed, however, instead of seven and the suspension springs and fastenings were made considerably stronger to withstand the higher loads. It was not possible, with a practical screen installation, to keep the Reynolds number of the flow around the wires of the screen below the critical value for viscous flow throughout the entire operating range of this tunnel. The wire size used (0.0065-inch diameter), however, allowed the tunnel to be operated below the critical Reynolds number of the wires up to a model Reynolds number of about 5.5×10^6 per foot of model chord. (See fig 10.) Upstream of the eleven 30-mesh screens, a 60-mesh screen was installed on a framework which supports the cooling coils described in the next section.

Turbulence measurements were made in August 1941 with the National Bureau of Standards hot-wire anemometer and typical results are shown in figure 2.

Cooling installation.- A finned cooling coil is located in the large section of the tunnel immediately upstream of the 60-mesh screen to control the temperature of the air stream. This cooling coil, which is 5 inches thick and covers the whole area of the air stream, contains a double row of copper tubes through which water from a cooling tower is passed at the rate of 1000 gallons per minute. In order to give a nearly uniform cooling distribution, the water enters some of the tubes from the top and others from the bottom. The coil is of adequate capacity to remove all the heat put into the air stream during full-power operation after a moderate rise in air-stream temperature.

In order to prevent extremely high humidity when the air in the tunnel is compressed, dehumidification of the air is necessary. This result is accomplished by a refrigeration unit in the test chamber containing coils for Freon-12 and water. Air from the tunnel is circulated through the refrigeration coils by a blower,

and the condensed moisture flows out of the tunnel through a drain trap. A relative humidity of about 50 percent is usually maintained.

The refrigeration unit also provides necessary cooling of the test chamber when the operating personnel are working inside. Additional coils for Freon-12, operating from the same refrigeration compressor as the coils in the test chamber, are installed in the air lock to provide cooling for personnel making entries into compressed air.

Blower equipment.- Auxiliary blower equipment consisting of three multistage centrifugal blowers, each driven by a 100-horsepower shunt-wound direct-current motor, is installed inside the tunnel test chamber. Each blower has a maximum capacity of 3950 cubic feet per minute with a pressure rise of 3.5 pounds per square inch at atmospheric pressure and a maximum capacity of 1720 cubic feet per minute with an 8.0-pound-per-square-inch pressure rise at 10 atmospheres.

The blower duct system is interconnected so that flexibility in the use of the blowers in tunnel operation is obtained. Either one or two of the blowers is used for boundary-layer control of the test-section wall and for control of the test-section longitudinal static-pressure gradient in a manner similar to that previously described for the test section of the Langley two-dimensional low-turbulence tunnel. The remaining blower or blowers are used for tests requiring an external air supply.

Model sizes.- Models tested in the Langley two-dimensional low-turbulence pressure tunnel usually completely span the 3-foot-wide test section. Chords of these models have ranged from 6 to 100 inches. In general, however, two ranges of chord size are used, namely, 24-inch chord (fig. 12) for standard lift, drag, and pitching-moment characteristics, and large-chord (70 to 90 inch) practical-construction models (fig. 13) for drag measurements over a small angular range near design lift. Model chords for the determination of maximum lift coefficients have been limited to 36 inches because of the effect of the tunnel walls on the pressure distributions of large models at high lift coefficients.

Methods of mounting models.- For almost all tests except those in which pitching moments are to be obtained, models are locked to the angle-of-attack mechanism and completely span the

tunnel test section with the ends of the model sealed to prevent air leakage. When pitching moments are to be obtained in the test, the model is mounted on a pitching-moment balance which is described in a subsequent section entitled, "Torque Balance for Moments."

Types of investigations to which tunnel is suited.- The Langley two-dimensional low-turbulence pressure tunnel, with the present equipment, is particularly suited for investigation of the effects of the basic variables of shape, camber, and surface condition on airfoil, flap, and control-surface characteristics at Reynolds numbers in or near the flight range of modern airplanes. These basic variables can be studied and evaluated from two-dimensional-flow data, which simplifies the problems to a great extent, because many complicating factors entering the three-dimensional tests are eliminated. Investigations are made with relatively inexpensive models of a size convenient for handling, and the results of the tests are quickly obtained with only a small amount of computation. Typical models are shown in figures 12, 13, and 14.

Investigations to find the aerodynamic characteristics of airfoils with air intakes and exits (fig. 15) or with boundary-layer control slots (fig. 16) can be easily made, and the wing-body interference effects of nacelles, fuselages, propellers, jets, and protuberances (fig. 17) can be determined at relatively high Reynolds numbers with models of a convenient size.

Methods of Measurement

A large part of the following discussion of methods of measurement is taken from the appendix of reference 9, which was written by M. M. Klein.

The lift and drag characteristics of airfoils tested in the Langley two-dimensional low-turbulence pressure tunnel are usually measured by methods not requiring the use of balances. The lift is evaluated from a measurement of pressure reactions on the floor and ceiling of the tunnel. The drag is obtained from measurements of static and total pressures in the wake of the airfoil. Moments are usually measured by a balance. These methods of measuring the forces on the model have the advantage that data can be easily reduced and tare corrections in the

usual sense, that is, forces acting on the model supports, are eliminated.

Measurement of lift.- The lift carried by the airfoil induces an equal and opposite reaction upon the floor and ceiling of the tunnel. The lift may therefore be obtained by integrating the pressure distribution along the floor and ceiling of the tunnel. This integration is made automatically with an integrating manometer described subsequently herein. Theoretically, the pressure field about the airfoil extends to infinity in both the upstream and downstream directions. All the lift is therefore not included in the finite length in the vicinity of the test section over which the integration is performed. The orifices in the floor and ceiling in the Langley two-dimensional low-turbulence pressure tunnel extend over a length of approximately 13 feet. The ratio of the measured lift to the actual lift for any lift distribution has been calculated theoretically. The calculation was made by finding the ratio of the measured lift to the actual lift of a two-dimensional point vortex situated at any position along the center line of the tunnel. A plot of this ratio η_x against position in the tunnel is given in figure 18. The ratio of the measured lift to the actual lift for any lift distribution η is found by determining the weighted average η_x over the chord of the model over the floor of the tunnel as follows:

$$\eta = \frac{\int_{\text{chord}} P_R \eta_x d\left(\frac{x}{c}\right)}{\int_{\text{chord}} P_R d\left(\frac{x}{c}\right)}$$

where P_R is the resultant pressure coefficient. The values of η_b and η_a for the Langley two-dimensional low-turbulence pressure tunnel are given in the following table where η_b is the η factor corresponding to the basic mean line load and η_a is the η factor for the additional type of load as given by thin-airfoil theory. The basic mean-line load of the airfoil is designated by the symbol a which denotes the fraction of the chord from the leading edge over which the design load is uniform (reference 9).

VALUES OF η_a AND η_b FOR LANGLEY TWO-DIMENSIONAL LOW-TURBULENCE PRESSURE TUNNEL

a \ c, ft	0.5	1.0	2.0	4.0	6.0	8.0
			η_b			
0	0.9320	0.9323	0.9322	0.9302	0.9251	0.9165
.1	.9320	.9323	.9323	.9303	.9253	.9168
.2	.9321	.9324	.9325	.9306	.9258	.9173
.3	.9322	.9325	.9328	.9310	.9262	.9177
.4	.9323	.9327	.9330	.9315	.9266	.9177
.5	.9324	.9329	.9333	.9318	.9267	.9172
.6	.9325	.9331	.9336	.9320	.9264	.9160
.7	.9326	.9333	.9339	.9322	.9258	.9140
.8	.9327	.9335	.9342	.9321	.9247	.9109
.9	.9328	.9337	.9345	.9318	.9231	.9066
1.0	.9330	.9339	.9347	.9314	.9209	.9010
			η_a			
------	0.9311	0.9307	0.9296	0.9254	0.9179	0.9068

The lift coefficient of the model in the tunnel uncorrected for blocking c_l' is given in terms of the lift coefficient measured in the tunnel c_{l_T} and the design lift coefficient of the airfoil c_{l_i} by the following equation:

$$c_l' = \frac{c_{l_T}}{\eta_a} - \left(\frac{\eta_b}{\eta_a} - 1\right)\left(c_{l_i}\right)$$

Inasmuch as η_b does not differ much from η_a, it is not necessary that the basic load or the design lift coefficient be known with great accuracy.

Because of tunnel-wall and other effects, the lift distribution over the airfoil in the tunnel does not agree exactly with the

assumed lift distribution, but because of the small variation of η with lift distribution, errors caused by this effect are considered negligible. Errors caused by neglecting the effect of airfoil thickness on the distribution of the lift reaction along the tunnel walls can also be shown to be small.

Measurement of drag.- The drag of an airfoil may be obtained from observations of the pressures in the wake (reference 10). An approximation to the drag is given by the loss in total pressure of the air in the wake of the airfoil. The loss of total pressure is measured by a rake of total-pressure tubes in the wake. The rake used in the Langley two-dimensional low-turbulence pressure tunnel is shown schematically in figure 19 and the survey apparatus for moving the rake in figure 20. When the total pressures in front of the airfoil and in the wake are represented by H_o and H_w, respectively, the drag coefficient c_{d_T} obtained from loss of total pressure is

$$c_{d_T} = \int_{wake} H_c \frac{dy_w}{c}$$

where

H_c coefficient of loss of total pressure in the wake $\left(\frac{H_o - H_w}{q_o}\right)$

y_w distance perpendicular to stream direction from position of $H_{c_{max}}$

If the static pressure in the wake is represented by p_w, the true drag coefficient uncorrected for blocking c_d' may be shown to be (reference 10)

$$c_d' = \int_{wake} 2\sqrt{S_w - H_c}\left(1 - \sqrt{1 - H_c}\right)\frac{dy_w}{c}$$

where S_w is the static-pressure coefficient in the wake $\left(\frac{H_o - p_w}{q_o}\right)$. The assumption is made that the variation of total pressure

across the wake can be represented by a normal probability curve. The drag coefficient c_d' is then easily obtainable from measurements of c_{d_T} by means of a factor K, the ratio of c_d' to c_{d_T}, which depends only on S_w and the maximum value of H_c. If the maximum value of H_c is represented by $H_{c_{max}}$, the equation of the normal probability curve is

$$H_c = H_{c_{max}} e^{-\left(\frac{By_w}{c}\right)^2}$$

where B is a dimensionless constant that determines the width of the wake. If a convenient variable of integration $Y = \frac{By_w}{c}$ is used, the ratio K is

$$K = \frac{c_d'}{c_{d_T}}$$

$$K = \frac{2}{\sqrt{\pi}} \frac{1}{H_{c_{max}}} \int_{-\infty}^{\infty} \sqrt{S_w - H_c} \left(1 - \sqrt{1 - H_c}\right) dY$$

and is independent of the width of the wake. The quantity K has been evaluated for various values of $H_{c_{max}}$ and S_w by assuming S_w to be constant across the wake. The drag coefficient c_d' may thus be obtained from tunnel measurements of c_{d_T}, $H_{c_{max}}$, and S_w. A plot of K as a function of $H_{c_{max}}$ with S_w as a parameter is given in figure 21. A parallel treatment of this problem is given in reference 11.

Torque balance for moments.- Pitching moments are measured in the Langley two-dimensional low-turbulence pressure tunnel by mounting the model on a torque-rod balance. This balance is shown schematically in figure 22. Deflection of the torque rod is amplified and indicated by a dial gage which is read by the

operators. The moment corresponding to the observed deflection of the dial gage is obtained from a calibration curve.

Calibration of the balance was made by hanging weights on an arm of known length attached to a stiff bar which was mounted on the balance in place of the model. The balance was calibrated for a range of moments from about 235 foot-pounds in the direction of positive airfoil pitching moments to 650 foot-pounds in the negative direction. A corresponding calibration curve was obtained for angular deflection of the balance so that the angle of attack of the model can be corrected.

Since it is necessary to mount the models with the ends clear of the tunnel walls, a method of sealing the gaps is necessary. For this purpose, rubber seals are attached to the ends of the model as shown in figure 23. These seals are inflated with air to seal the gaps when moment readings are taken and deflated when the angle of attack is changed. Negligible errors in moment readings result from the use of the rubber seals since a large part of the deflection of the torque rod occurs before the seals are inflated; and after the seals are inflated, any additional deflection resulting from a change in moment due to sealing the ends of the model causes a rolling action of the seals, which offers very little resistance to small movements.

Principles of integrating manometers.- Integrating manometers are used in both of the Langley two-dimensional low-turbulence tunnels to measure lift and drag. In the case of the drag measurements, the integrating manometer gives an indication of the integral $\int_{wake} (H_o - H_w)\ dy$, a first approximation to the drag,

where

H_o free-stream total pressure

H_w total pressure indicated by individual tube in wake

In the case of the lift measurements, two integrating manometers are used to evaluate the following integrals:

$$\int_L (p_r - p_U)\ dL$$

$$\int_L (p_r - p_L)\ dL$$

where

p_r reference pressure

p_U static pressure at any point on the ceiling within the length L

p_L static pressure at any point on the floor within the length L

Each integrating manometer consists of a group of calibrated tubes having uniform bores of equal diameters connected rigidly to a common manifold and filled with liquid to a convenient level. Figure 24 shows the arrangement schematically. The liquid level in one tube, called the integrating tube, is read with a micrometer microscope to obtain a sufficiently accurate reading. This integrating tube, together with one or more other tubes of the manometer, is connected to a suitable reference pressure. For the drag measurements, this pressure is the free-stream total pressure. For the lift measurements, it is an arbitrary reference pressure. The values of the aforementioned integrals are obtained by observing the change in level of the integrating tube that occurs when a pressure distribution is applied to the manometer.

The basic relations for the integrating manometers may be derived as follows: Let

p_r reference pressure

$p_{1,2,\ldots i}$ pressure applied to individual tube

ΔL distance between uniformly spaced pressure orifices

n number of individual tubes in integrating manometer or individual pressure orifices (tubes not acted upon by reference pressure)

k ratio of combined area of tubes connected to reference pressure to the area of a tube connected to an individual orifice

A area of individual manometer tube

a height of liquid when same pressure is applied to all tubes

b height of liquid in integrating tube when pressure distribution is applied to manometer and reference pressure p_r is applied to integrating and reference tubes

$h_{1,2,\ldots i}$ height of liquid in any individual tube when pressure distribution is applied

The volume of liquid above the level b when a pressure distribution is applied to the manometer is equal to $\sum_{1}^{n}(h_i - b)A$ and the volume of liquid above the level b when the pressure on all tubes is the same is equal to $(n + k)A(a - b)$. Because the total volume of liquid in the manometer is constant

$$\sum_{1}^{n}(h_i - b) = (n + k)\ (a - b)$$

The deflection of each individual tube $(h_i - b)$ is proportional to the pressure difference $(p_r - p_i)$ or $\rho(h_i - b) = p_r - p_i$ where ρ is the density of manometer liquid. Hence,

$$\sum_{1}^{n}(p_r - p_i)\Delta L = \rho(n + k)\ (a - b)\Delta L$$

If the spacing of the individual orifices is sufficiently close, then for the lift integrating manometer

$$\int_{L}(p_r - p_i)\ dL = \rho(n + k)\ (a - b)\ \Delta L$$

or, in the case of the drag manometer,

$$\int_{\text{wake}}(H_o - H_w)\ dy = \rho(n + k)\ (a - b)\ \Delta y$$

where Δy is the spacing of the total pressure tubes in the rake. The corresponding drag coefficient c_{d_T} is found by dividing this integral by the dynamic pressure q_o' and the chord of the model c. The dynamic pressure q_o' is usually found from the deflection Δp_{SP} of another manometer using the same liquid as the integrating manometer as follows:

$$q_o' = f_{SP} \Delta p_{SP} \rho$$

where f_{SP} is a calibration factor for Δp_{SP}. Hence

$$c_{d_T} = \frac{(n + k)(a - b)\Delta y}{f_{SP} \Delta p_{SP} c}$$

The relations when the integrating manometers are applied to the measurement of lift may be derived by a similar process.

Tunnel-Wall Corrections

As discussed by M. M. Klein in the appendix of reference 9, in two-dimensional flow, the tunnel walls may be conveniently considered as having two distinct effects upon the flow over a model in the tunnel:

(1) An increase in the free-stream velocity in the neighborhood of the model because of a constriction of the flow

(2) A distortion of the lift distribution from the induced curvature of the flow

The increase in free-stream velocity caused by the tunnel walls (blocking effect) is obtained from consideration of an infinite vertical row of images of a symmetrical body as given in reference 12; the images represent the effect of the tunnel walls. For convenience in tunnel calculations, the expression for ΔV, the increment of tunnel velocity caused by blocking, may be written

$$\frac{\Delta V}{V} = K\sigma$$

where

$$\sigma = \frac{\pi^2}{48}\left(\frac{c}{h_T}\right)^2$$

wherein c is model chord and h_T the tunnel height. The factor σ depends only on the size of the body. The factor Λ depends on the shape of the body. The value of Λ may be obtained from the velocity distribution over the body by the expression

$$\Lambda = \frac{16}{\pi}\int_0^1 \frac{y}{c}\frac{v}{V}\sqrt{1 + \left(\frac{dy_t}{dx}\right)^2}\, d\frac{x}{c}$$

where v is the velocity at any point on the surface and dy_t/dx is the slope of the surface at any point at which the ordinate is y_t.

In addition to the error caused by blocking, an error exists in the measured tunnel velocity because of the interference effects of the model upon the velocity indicated by the static-pressure orifices located in the vertical walls a few feet upstream of the model and half way between the floor and ceiling. In order to correct for this error, an analysis was made of the velocity distribution along the streamline half way between the upper and the lower tunnel walls for Rankine ovals of various sizes and thickness ratios. The analysis showed that the correction could be expressed, within the range of conventional-airfoil thickness ratios, as a product of a thickness factor given by the blocking factor Λ and a factor ξ which depends upon the size of the model and the distance from the static-pressure orifices to the midchord point of the model. The corrected indicated tunnel velocity V' could then be written

$$V' = V''(1 + \Lambda\xi)$$

where V'' is the velocity measured by the static-pressure orifices. In the Langley two-dimensional low-turbulence tunnels, for a model having a chord of 2 feet, the distance from the static-pressure orifices to the midchord point of the model is approximately 5.5 feet, and the corresponding value of ξ is approximately 0.002.

In order to calculate the effect of the tunnel walls upon the lift distribution, a comparison is made of the lift distribution of a given airfoil in a tunnel and in free air on the basis of thin-airfoil theory. It is assumed that the flow conditions in the tunnel correspond most closely to those in free air when the additional lift in the tunnel and in free air are the same (reference 13). On this basis, the following corrections are derived (reference 13), in which the primed quantities refer to the coefficients measured in the tunnel:

$$c_l = [1 - 2\Lambda(\sigma + \xi) - \sigma]\, c_l'$$

$$\alpha_o = (1 + \sigma)\alpha_o' + \frac{4\sigma c_{m_{c/4}}'}{dc_l'/d\alpha_o'} = \sigma\alpha_{l_o}$$

$$c_{m_{c/4}} = [1 - 2\Lambda(\sigma + \xi)]\, c_{m_{c/4}}' + \sigma\frac{c_l'}{4}$$

In the foregoing equations, the terms $\frac{4\sigma c_{m_{c/4}}'}{dc_l'/d\alpha_o'}$, α_{l_o}, and $\sigma c_l'/4$ are usually negligible for 2-foot-chord models in the Langley two-dimensional low-turbulence tunnels.

When the effect of the tunnel walls on the pressure distribution over the model is small, the wall effect on the drag is merely that corresponding to an increase in the tunnel speed. The correction to the drag coefficient is, therefore, given by the following relation:

$$c_d = [1 - 2\Lambda(\sigma + \xi)]\, c_d' \qquad (1)$$

Similar considerations have been applied to the development of the corrections for the pressure distribution in reference 13.

Equation (1) neglects the blocking due to the wake, such blocking being small at low to moderate drags. The effect of a pressure gradient in the tunnel upon loss of total pressure in the wake is not easily analyzed but is estimated to be small. The effect of pressure gradient upon the drag has, therefore, been disregarded. When the drag is measured by a balance, the effect of the pressure gradient upon the drag is directly additive and a correction should be applied. For large models, especially at high lift coefficients, the effect of the tunnel walls is to distort the pressure distribution appreciably. Such distortions of the pressure distribution may cause large changes in the boundary flow and no adequate corrections to any of the coefficients, particularly the drag, can be found.

Correction for blocking at high lifts.- So long as the flow follows the airfoil surface, the foregoing relations account for the effects of the tunnel walls with sufficient accuracy. When the flow leaves the surface, the blocking increases because of the predominant effect of the wake upon the free-stream velocity. Since the wake effect shows up primarily in the drag, the increase in blocking would logically be expressed in terms of the drag. The accurate measurement of drag under these conditions by means of a rake is impractical because of spanwise movements of low-energy air. A method of correcting for increased blocking at high angles of attack without drag measurements has therefore been devised for use in the Langley two-dimensional low-turbulence tunnels.

Readings to indicate the floor and ceiling velocities are taken a few inches ahead of the quarter-chord point and averaged to remove the effect of lift. This average F, which is a measure of the effective tunnel velocity, is essentially constant in the low-lift range. The quantity F/F_o, where F_o is the average of F in the low-lift range, however, shows a variation from unity in the high-lift range for any airfoil tested at high lifts. A plot of F/F_o against angle of attack α_o' for a 2-foot-chord model of the NACA 64_3-418 airfoil is given in figure 25. The quantity F/F_o is nearly constant for values of α_o' up to 12°; but for values of α_o' greater than 12°, F/F_o increases, and the increase is particularly noticeable at and over the stall.

A theoretical comparison was made of the blocking factor $\Lambda\sigma$, and the velocity measured by the floor and ceiling orifices for a series of Rankine ovals of various sizes and thickness ratios. The quarter-chord point of each oval was located at the pivot point, the usual position of an airfoil in the tunnel. The analysis showed the relation between the blocking factor $\Lambda\sigma$ and the change in F to be unique for chord lengths up to 50 inches in that different

bodies having the same blocking factor $\Lambda\sigma$ gave approximately the same value of F. For chords up to 50 inches, the relationship is

$$\frac{\Delta V}{V} = 0.45\left(\frac{F}{F_o} - 1\right) \qquad (2)$$

where $\Delta V/V$ is the increment in tunnel velocity due to blocking. The foregoing relation was adopted to obtain the correction to the blocking in the range of lifts where $\frac{F}{F_o} > 1$.

Considerable uncertainty exists regarding the correct numerical value of the coefficient occurring in equation (2). If a row of sources, rather than the Rankine ovals used in the present analysis, is considered to represent the effect of the wake, the value of the coefficient in equation (2) would be approximately twice the value used. Fortunately, the correction amounts to only about 2 percent at maximum lift for an extreme condition with a 2-foot-chord model. Further refinement of this correction has, therefore, not been attempted.

Comparison with experiment.- A check of the validity of the tunnel-wall corrections has been made in reference 13, which gives lift and moment for models having various ratios of chord to tunnel height, uncorrected and corrected for tunnel-wall effects. The general agreement of the corrected curves shows that the method of correcting the lifts and moments is valid.

A comparison is made in reference 13 between the theoretical correction factor (equation (1)) and the experimentally derived corrections of reference 14. The theoretical correction factors were found to be in good agreement with those obtained experimentally.

In order to check the validity of the η-factor, a comparison has been made of lift values obtained from pressure distributions with those obtained from the integration of the floor and ceiling pressures in the tunnel. A comparison for two airfoils given in figure 26 shows that the two methods of measuring lift give results that are in good agreement. The η-factor has also been checked by comparison of the lift obtained from balance measurements with the integrating manometer values in figure 27.

Finally, a check has been made of the method of correcting pressure distributions (reference 13) for NACA 6-series airfoils of two chord lengths at zero angle of attack in figure 28, in which the pressure coefficients are plotted against chordwise

position x/c. The agreement between the corrected pressure distributions for both models verifies the method of making the tunnel-wall corrections.

Typical Results

Standard airfoil characteristics.- Figure 29, which gives the aerodynamic characteristics of the NACA 64_2-215 airfoil section, shows the type and range of data obtained in a standard airfoil test of a 24-inch-chord model (fig. 12) in the Langley two-dimensional low-turbulence pressure tunnel. These results are typical of those presented in reference 9 for a large number of airfoils tested in this wind tunnel.

The Reynolds number range of 3 to 9×10^6 was selected for convenience in testing since these Reynolds numbers can be reached with 24-inch chord models at air pressures which are not above the limit allowed for personnel to enter the tunnel under pressure to inspect models. Tests can also be made more quickly using these lower air pressures. These Reynolds numbers are within the landing Reynolds number range of many airplanes, and it is thought that sufficient indication of the scale effect on the airfoil characteristics is obtained for application to larger airplanes.

Since it is realized that airplanes do not usually operate with aerodynamically smooth surfaces on the wings, standard airfoil section characteristics (as shown in fig. 29) are obtained both with smooth model surfaces and with roughness particles around the leading edge to simulate a condition of an airplane wing surface somewhat rougher than that usually caused by manufacturing irregularities or deterioration in service, but not so rough as that usually encountered under icing conditions or through damage as in battle.

Tests of airfoil section models with simulated 60° split trailing-edge flaps are also included in the standard airfoil characteristics shown in figure 29. It is believed that these data will give an indication of the effectiveness of a more powerful trailing-edge high-lift device although sufficient data to verify this assumption have not been obtained.

Drag characteristics at high Reynolds numbers.- The drag characteristics of a number of models having chords larger than 24 inches have been obtained in the Langley two-dimensional low-turbulence pressure tunnel over a limited range of lift coefficient. Figure 30 shows drag data from a typical test of a medium

size model having surfaces which were smooth and almost free from waviness. Tests such as this have tended to support the belief that the Reynolds number range covered by standard airfoil tests in this wind tunnel is usually sufficient to give an indication of the variation of some of the airfoil characteristics at higher Reynolds numbers.

Large chord practical-construction wing sections (fig. 13) have been tested over a wide range of Reynolds numbers extending to very high values to determine the drag characteristics in the angular range near design lift. (See reference 15.) Studies are usually made of the effects of various surface finishes on the drag characteristics, and attempts are made to improve the characteristics by finishing methods which might be practical for a manufacturer to use in actual production. Figure 31 shows the results of tests of a wing section of this type with two surface conditions.

Comparison with flight measurements.- Several tests have been made in the Langley two-dimensional low-turbulence pressure tunnel which indicate reasonably good agreement between data obtained in this tunnel and in flight. Figure 32 gives a comparison between drag coefficients measured in flight and in the wind tunnel. For the flight measurements, an airfoil section model having a chord of four feet and a span of about six feet was mounted on an airplane. For the wind-tunnel tests, a part of this panel was used. Measurements were made at the same spanwise position for both tests, and surface conditions were as nearly the same as possible. As shown in figure 32 drag coefficients measured in the wind tunnel, although slightly higher than those measured in flight, are considered to agree very well in the range tested.

Although no direct comparison between airfoil boundary-layer measurements made in flight and in the Langley two-dimensional low-turbulence pressure tunnel is available, several tests and calculations indicate that airfoil boundary-layer conditions equivalent to those of flight may be obtained in this wind tunnel under some conditions. Boundary-layer measurements in flight of a specially built-up test panel having an airfoil section which would permit extensive laminar boundary layers indicated values of R_δ of 7500 to 9000. (See reference 3.) By use of a value of R_δ of 9000, drag coefficients were calculated for an airfoil tested in this wind tunnel, and the results of the calculations are shown in figure 31, together with experimental results for the same airfoil. It can be seen that the results

closely agree. These results seem to indicate that values of R_δ comparable with those obtained in flight existed for this model in the wind-tunnel test.

More direct comparisons of airfoil characteristics from the results of flight tests and tests in the Langley two-dimensional low-turbulence pressure tunnel are difficult to make because of the complications of different surface conditions and other factors which influence the airfoil characteristics to such an extent that accurate conclusions can not be reached.

Langley Memorial Aeronautical Laboratory
National Advisory Committee for Aeronautics
Langley Field, Va. January 22, 1947

REFERENCES

1. Jacobs, Eastman N., and Abbott, Ira H.: Airfoil Section Data Obtained in the N.A.C.A. Variable-Density Tunnel as Affected by Support Interference and Other Corrections. NACA Rep. No. 669, 1939.

2. Anderson, Raymond F.: The Experimental and Calculated Characteristics of 22 Tapered Wings. NACA Rep. No. 627, 1938.

3. Wetmore, J. W., Zalovcik, J. A., and Platt, Robert C.: A Flight Investigation of the Boundary-Layer Characteristics and Profile Drag of the NACA 35-215 Laminar-Flow Airfoil at High Reynolds Numbers. NACA MR, Air Corps, May 5, 1941.

4. Robinson, Russell G.: Sphere Tests in the N.A.C.A. 8-Foot High-Speed Tunnel. Jour. Aero. Sci., vol. 4, no. 5, March 1937, pp. 199-201.

5. Platt, Robert C.: Turbulence Factors of N.A.C.A. Wind Tunnels as Determined by Sphere Tests. NACA Rep. No. 558, 1936.

6. Becker, John V.: Boundary-Layer Transition on the N.A.C.A. 0012 and 23012 Airfoils in the 8-Foot High-Speed Wind Tunnel. NACA ACR, Jan. 1940.

7. von Doenhoff, Albert E.: Investigation of the Boundary Layer about a Symmetrical Airfoil in a Wind Tunnel of Low Turbulence. NACA ACR, Aug. 1940.

8. Taylor, G. I.: Statistical Theory of Turbulence. Parts I and II. Proc. Roy. Soc. (London), ser. A vol. 151, no. 873, Sept. 2, 1935, pp. 421-454.

9. Abbott, Ira H., von Doenhoff, Albert E., and Stivers, Louis S., Jr.: Summary of Airfoil Data. NACA ACR No. L5C05, 1945.

10. The Cambridge University Aeronautics Laboratory: The Measurement of Profile Drag by the Pitot-Traverse Method. R. & M. No. 1688, British A.R.C., 1936.

11. Silverstein, A., and Katzoff, S.: A Simplified Method for Determining Wing Profile Drag in Flight. Jour. Aero. Sci., vol. 7, no. 7, May 1940, pp. 295-301.

12. Glauert, H.: Wind Tunnel Interference on Wings, Bodies and Airscrews. R. & M. No. 1566, British A.R.C., 1933.

13. Allen, H. Julian, and Vincenti, Walter G.: The Wall Interference in a Two-Dimensional-Flow Wind Tunnel with Consideration of the Effect of Compressibility. NACA Rep. No. 782, 1944.

14. Fage, A.: On the Two-Dimensional Flow past a Body of Symmetrical Cross-Section Mounted in a Channel of Finite Breadth. R. & M. No. 1223, British A.R.C., 1929.

15. Quinn, John H., Jr.: Summary of Drag Characteristics of Practical-Construction Wing Sections. NACA TN No. 1151, 1947.

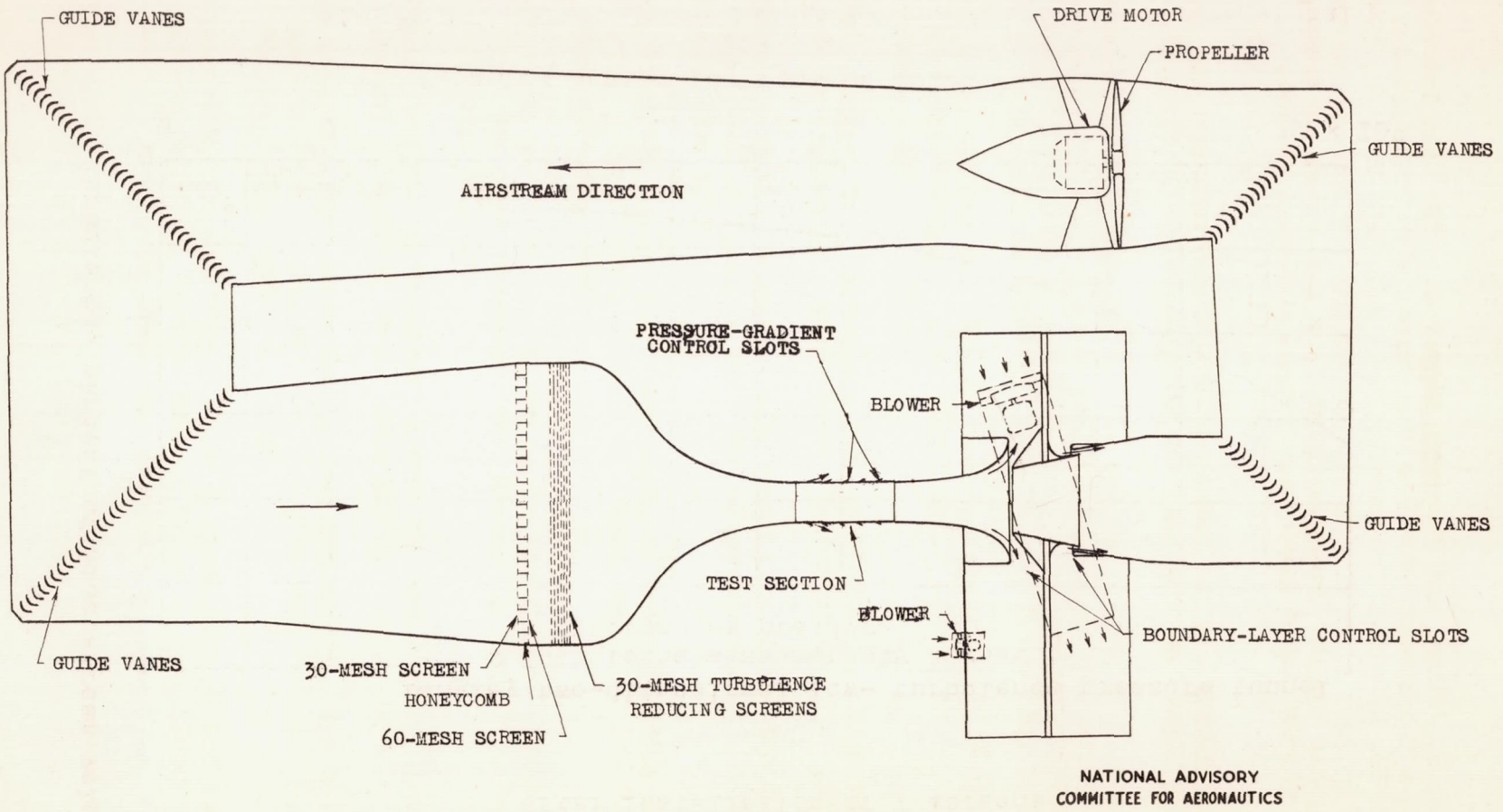

Figure 1.- Line drawing of the Langley two-dimensional low-turbulence tunnel.

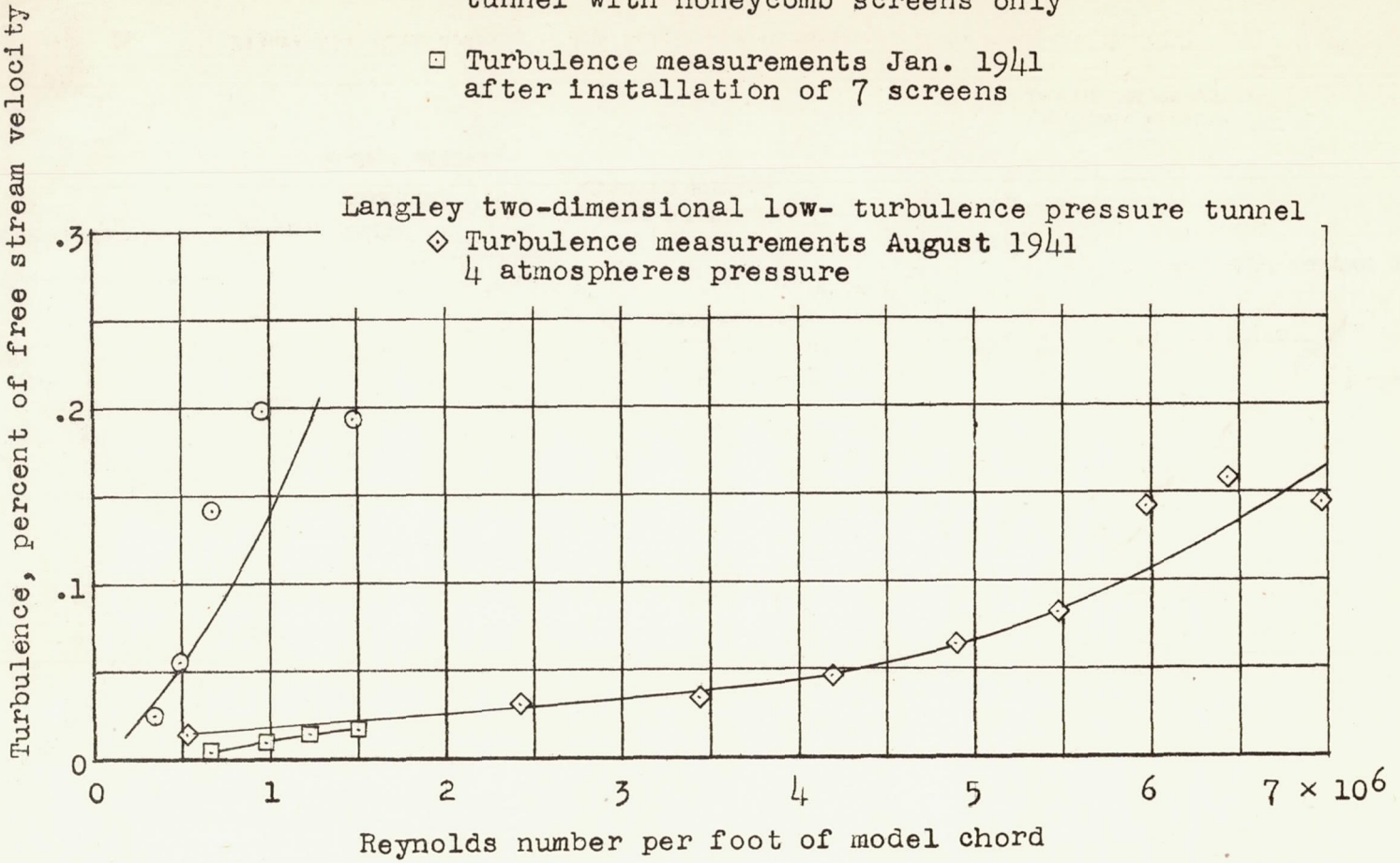

Figure 2 .- Turbulence levels of the Langley two-dimensional low-turbulence tunnels.

NATIONAL ADVISORY
COMMITTEE FOR AERONAUTICS

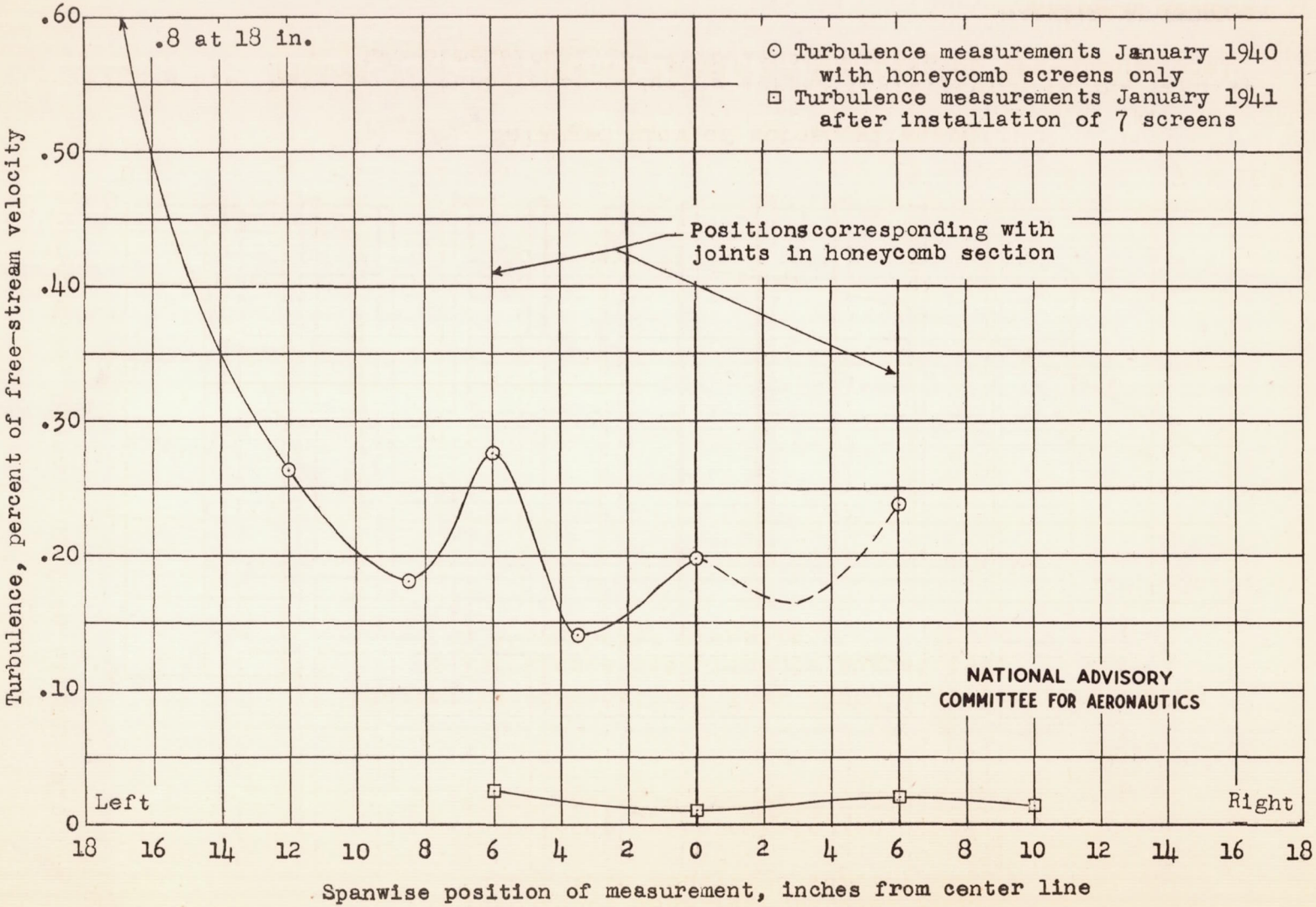

Figure 3.- Turbulence level of the Langley two-dimensional low-turbulence tunnel (speed approximately 100 miles per hour).

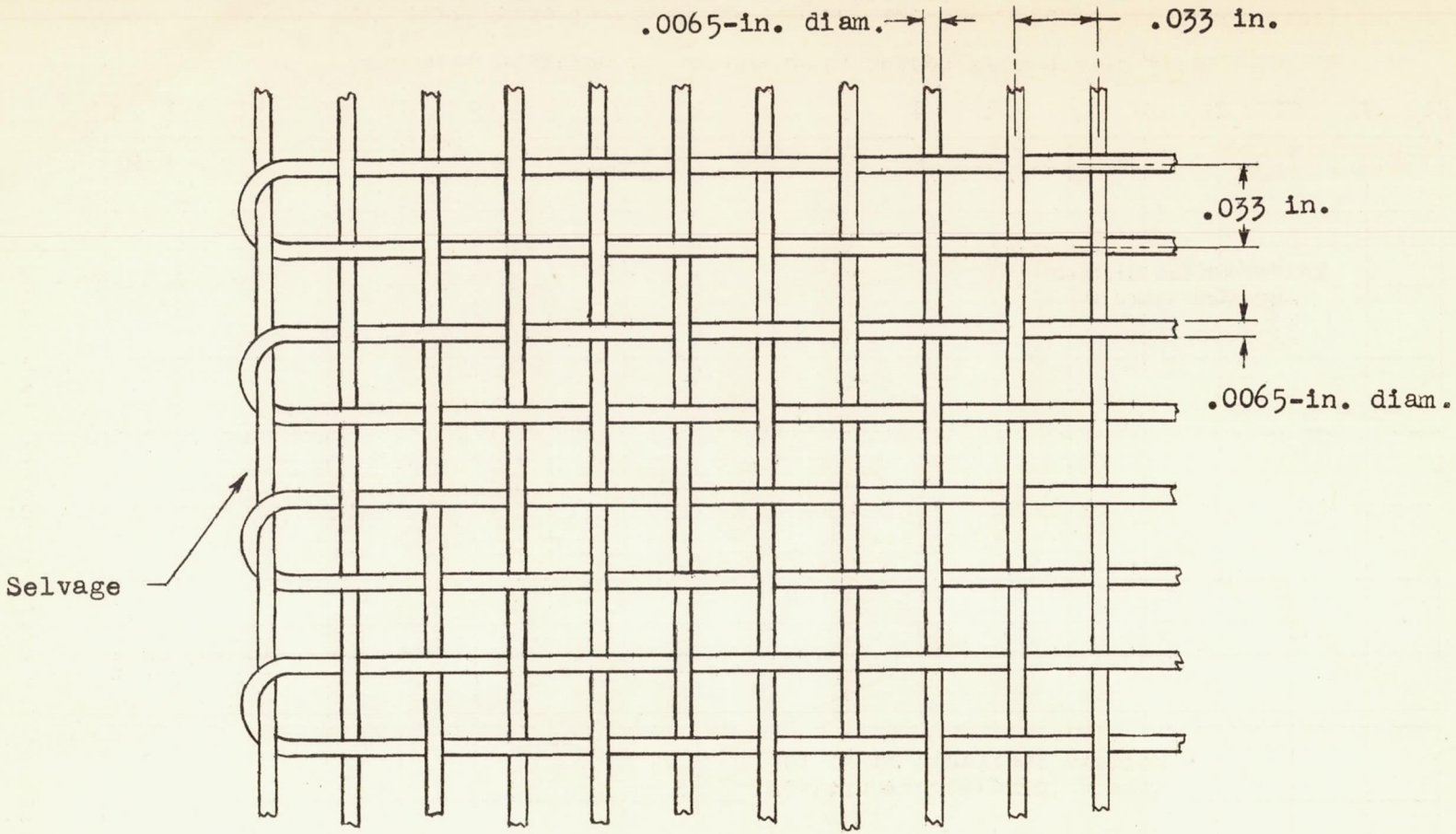

(a) Enlarged view of screen wire.

Figure 4.- Details of turbulence-reducing screen installation in the Langley two-dimensional low-turbulence tunnels.

NATIONAL ADVISORY
COMMITTEE FOR AERONAUTICS

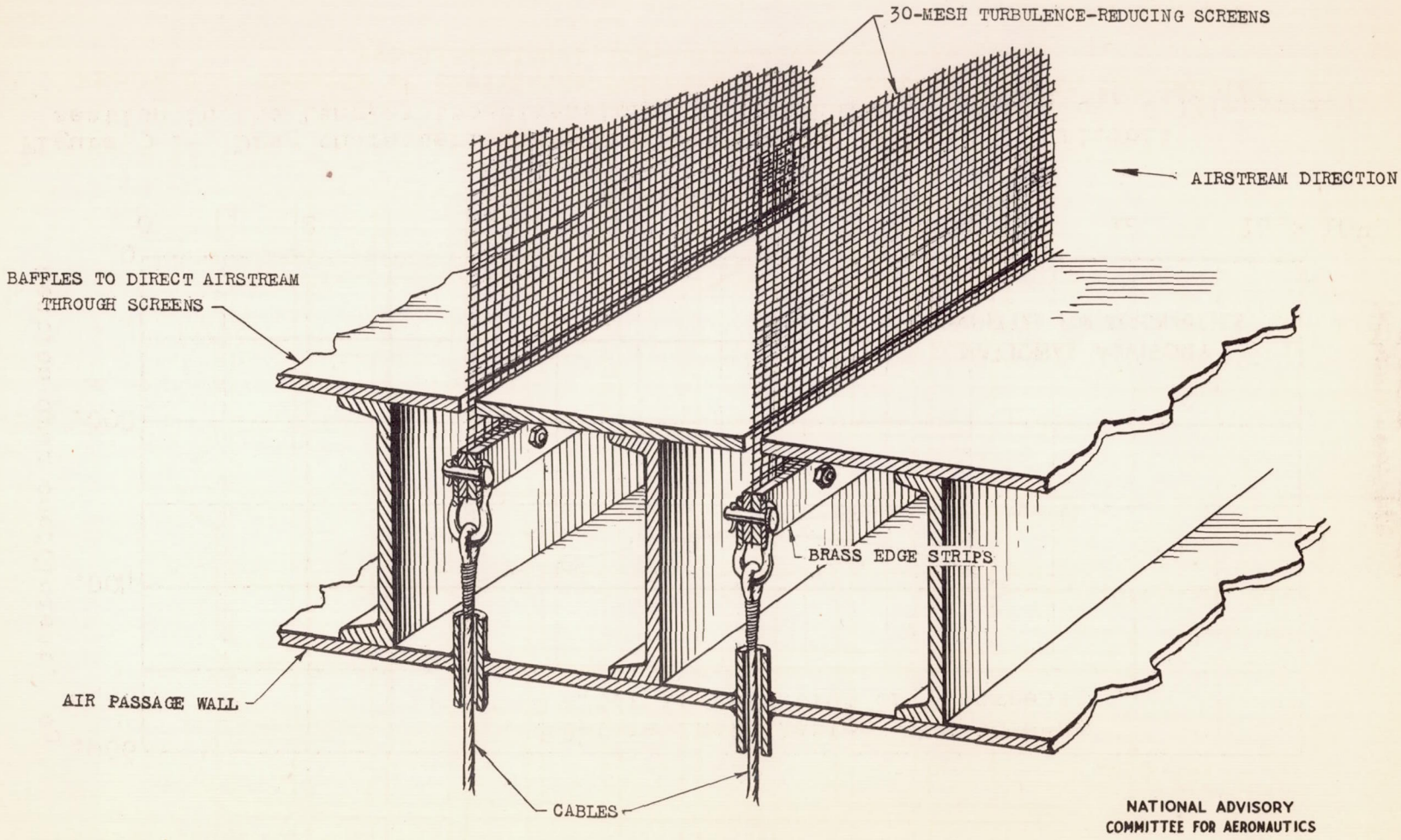

(b) Typical section through ends of screens showing edge strips and baffles.

Figure 4.- Concluded.

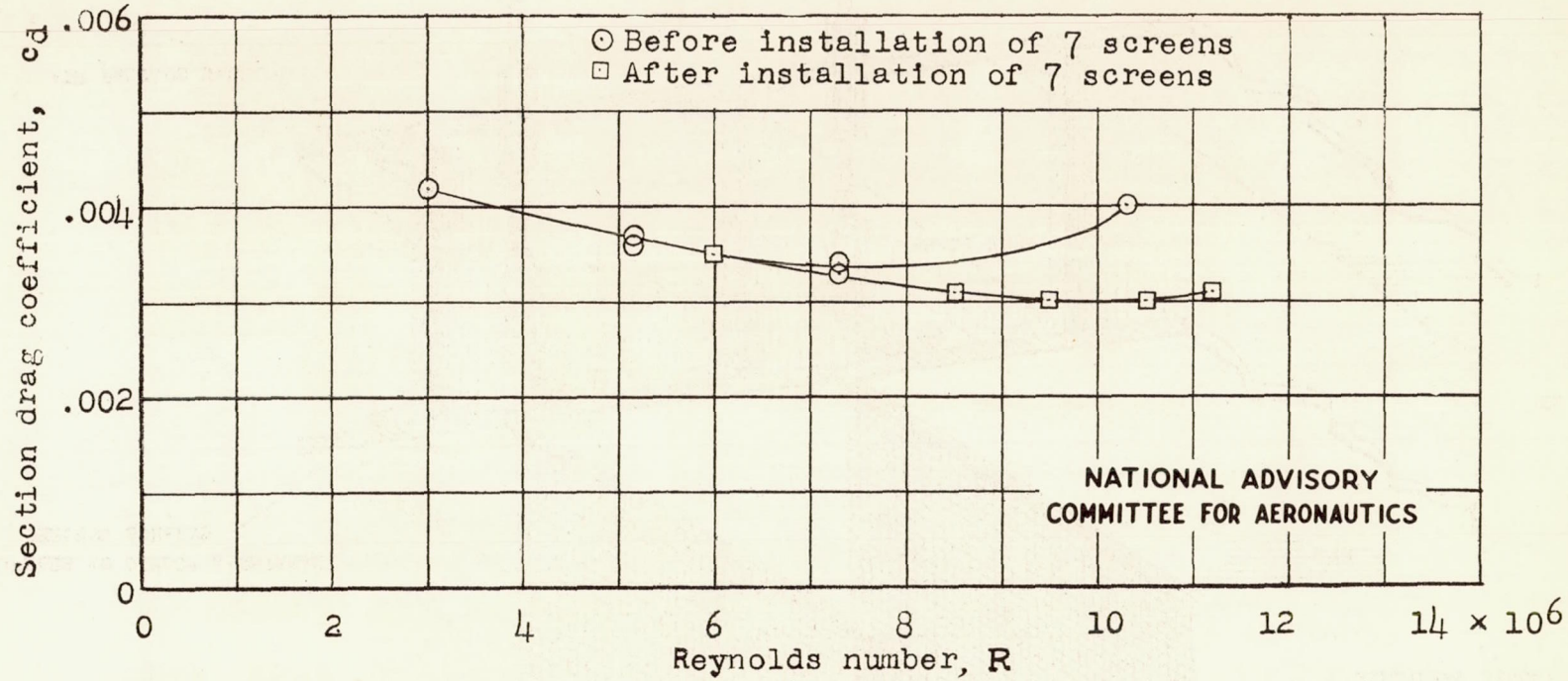

Figure 5 .- Drag characteristics of 90-inch chord NACA 67-215 airfoil section in the Langley two-dimensional low-turbulence tunnel. c_l, 0.13(approx.).

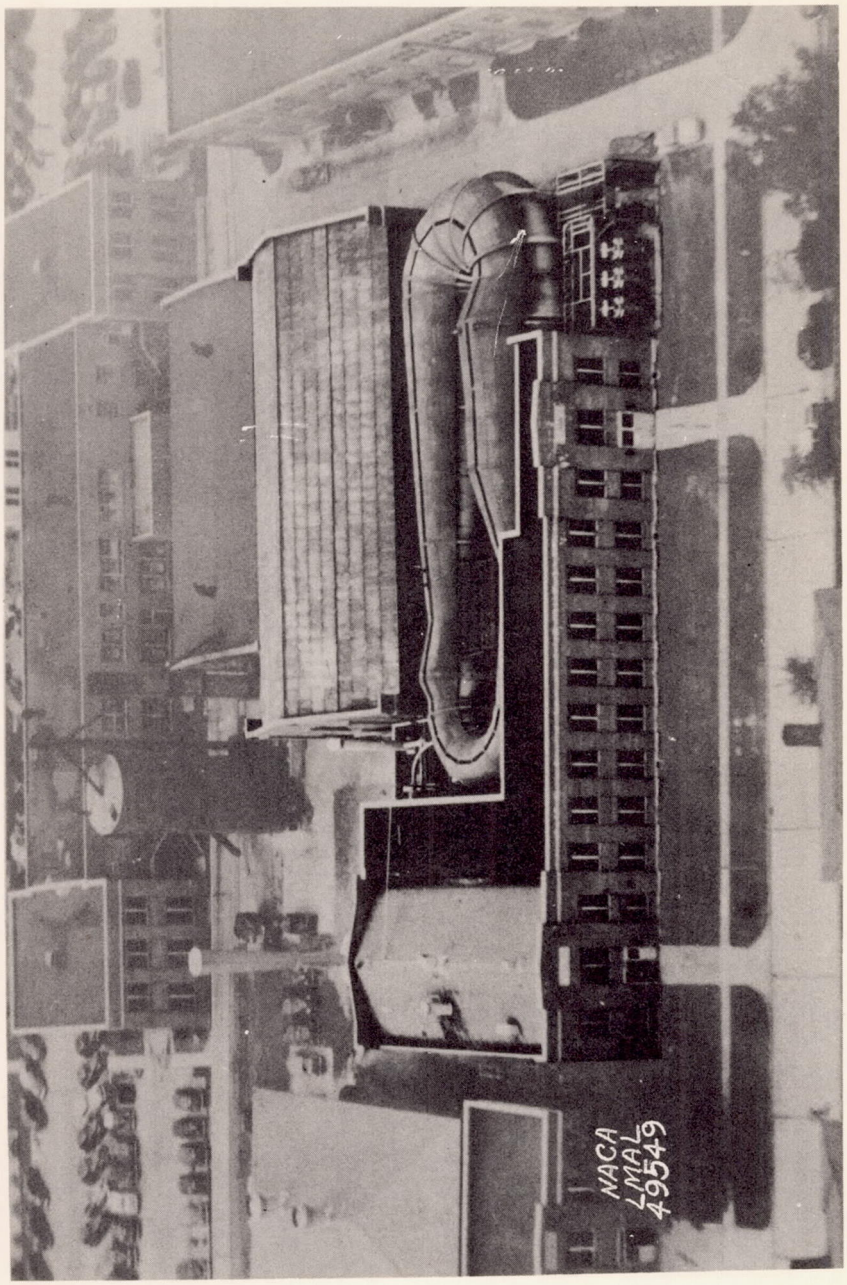

Figure 6.- The Langley two-dimensional low-turbulence pressure tunnel.

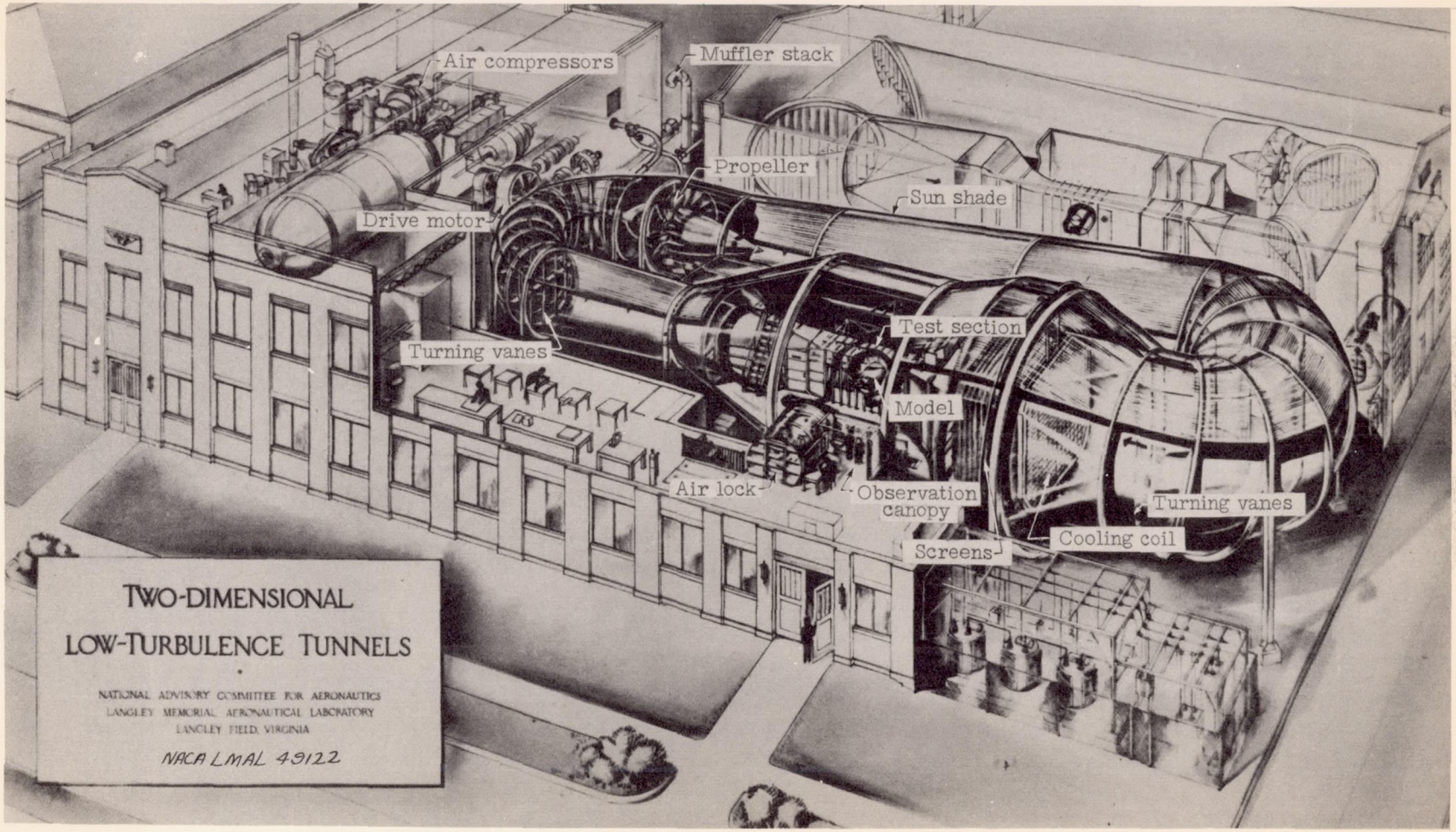

(a) Phantom drawing of the tunnel and related equipment.

Figure 7.- Drawings of the Langley two-dimensional low-turbulence pressure tunnel.

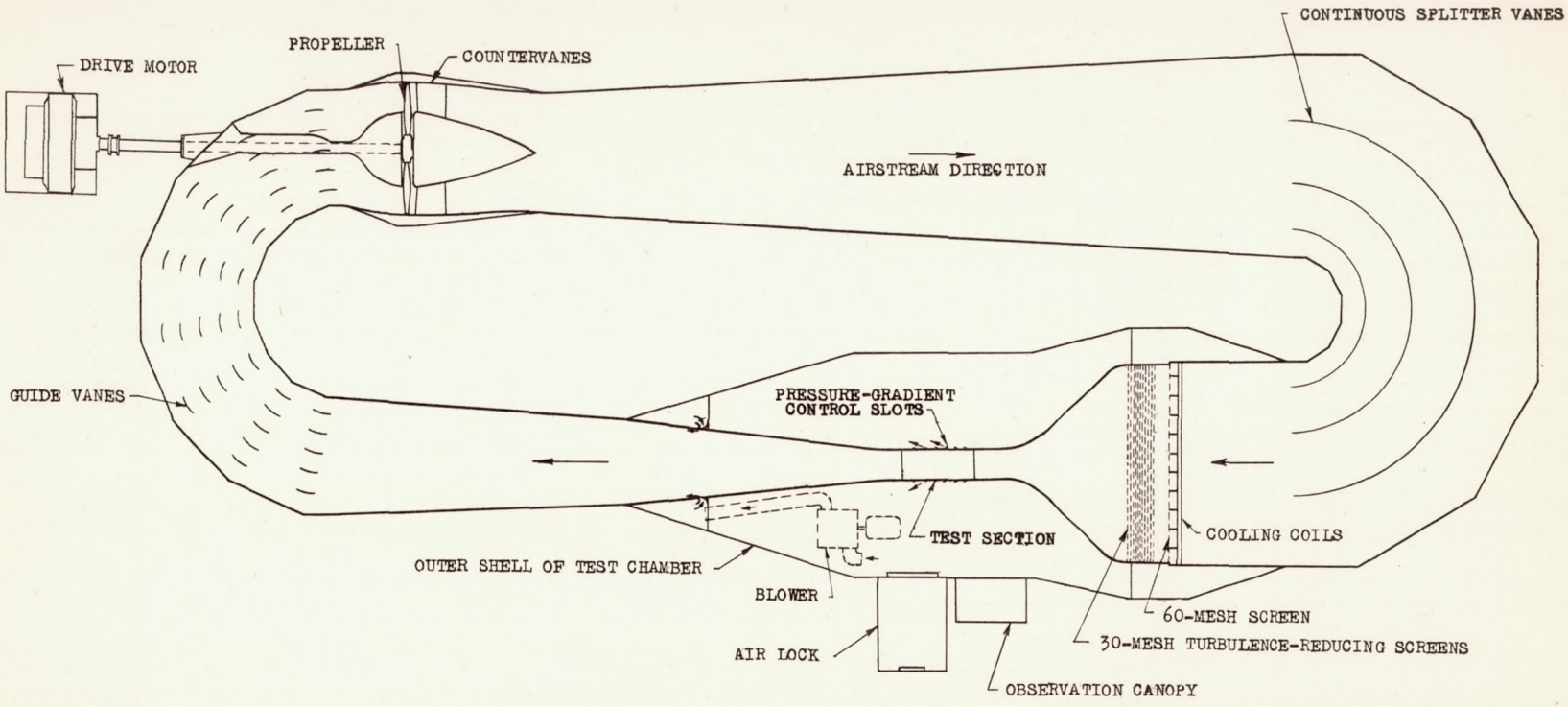

(b) Line drawing of the tunnel.

Figure 7.- Concluded.

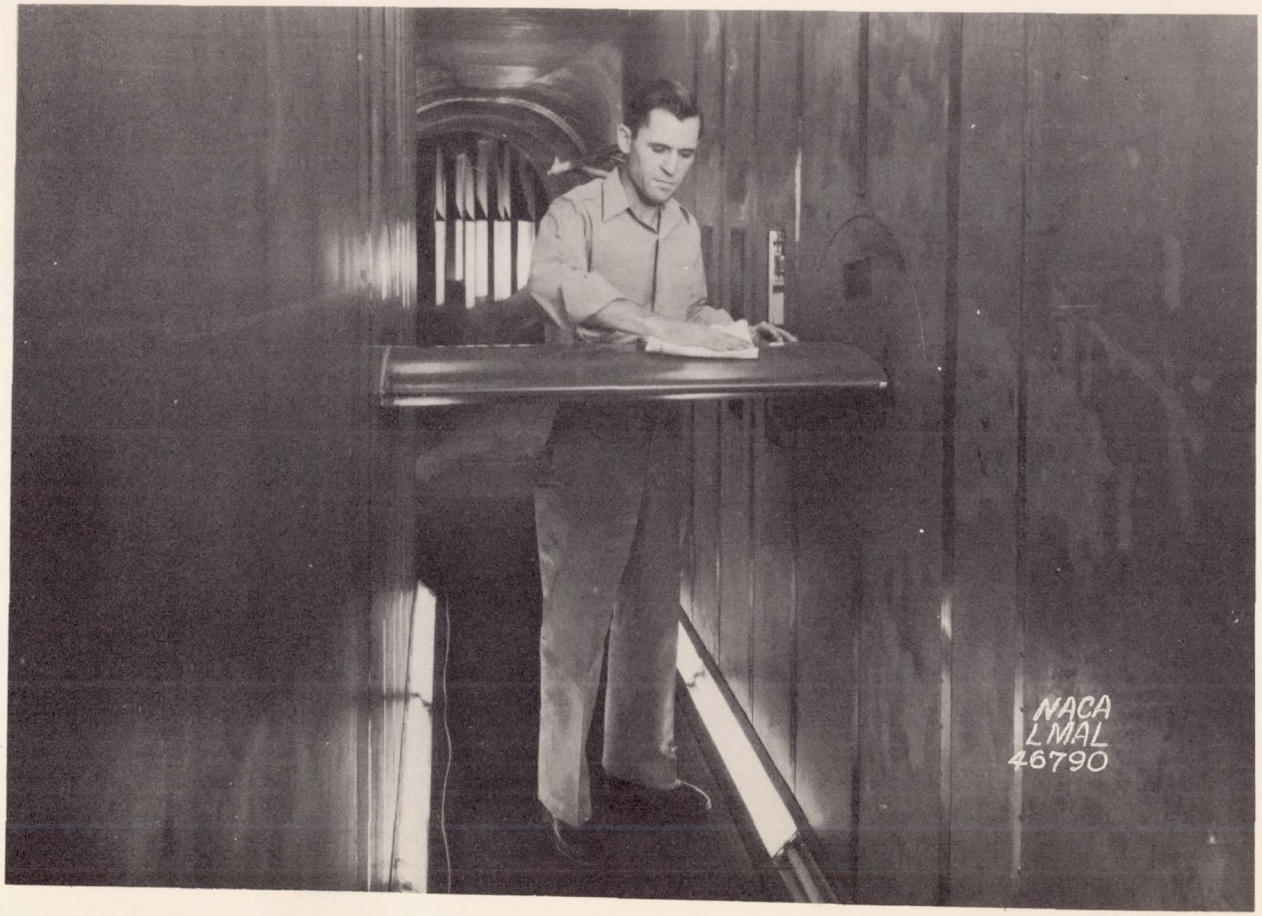

Figure 8.- Airfoil model in the test section of the Langley two-dimensional low-turbulence pressure tunnel (looking downstream).

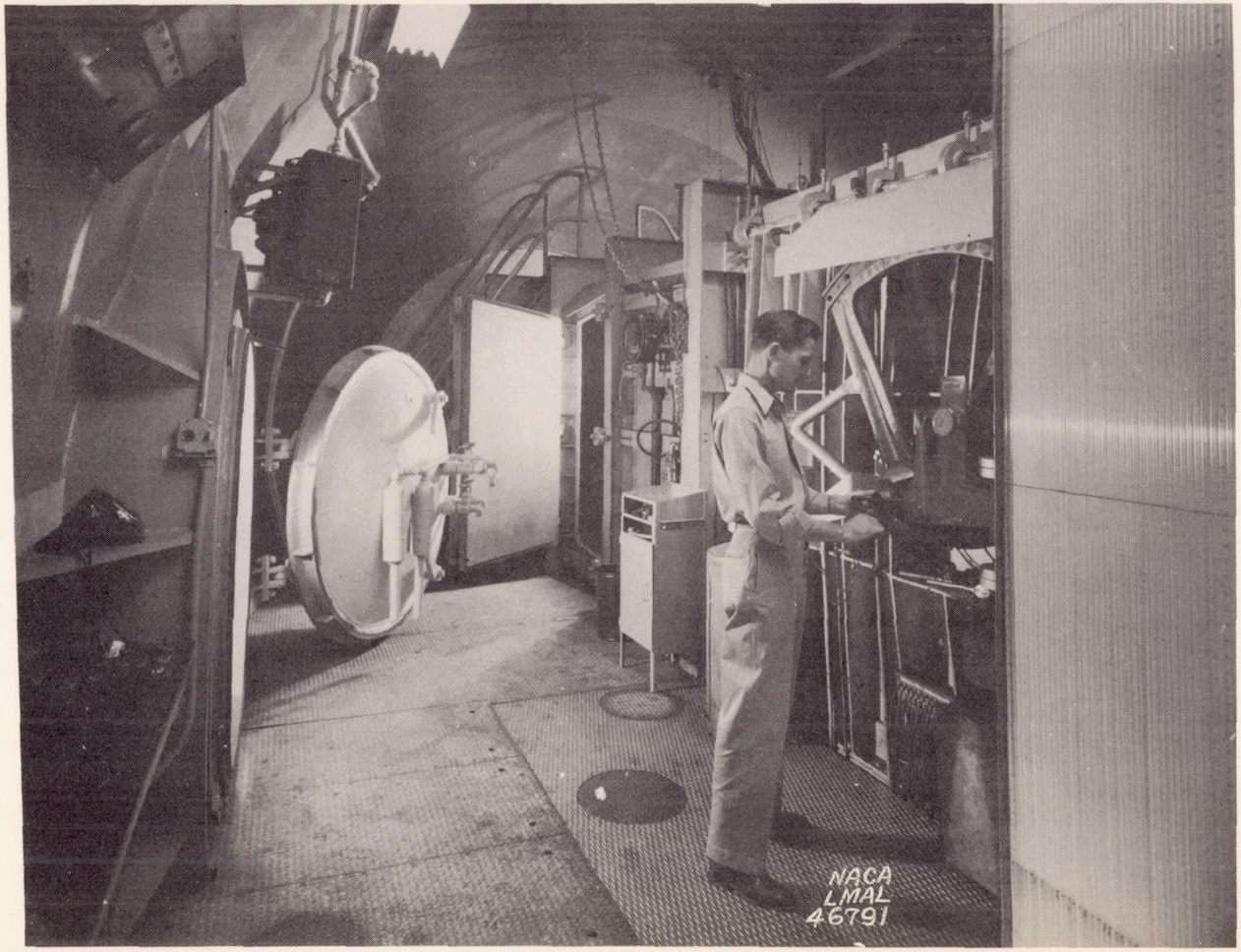

Figure 9.- Test chamber of the Langley two-dimensional low-turbulence pressure tunnel.

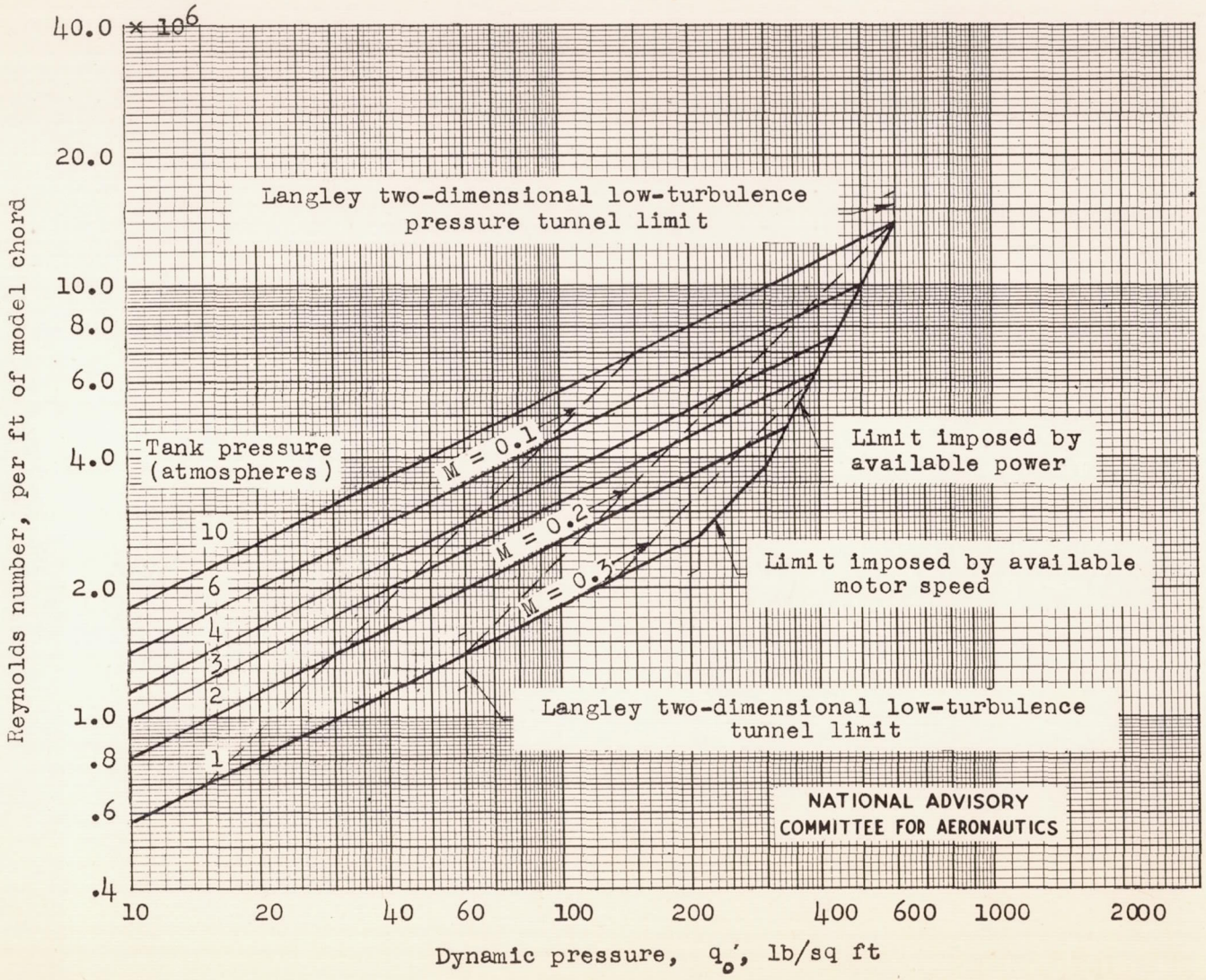

Figure 10 .- Reynolds number and dynamic-pressure ranges of the Langley two-dimensional low-turbulence tunnels.

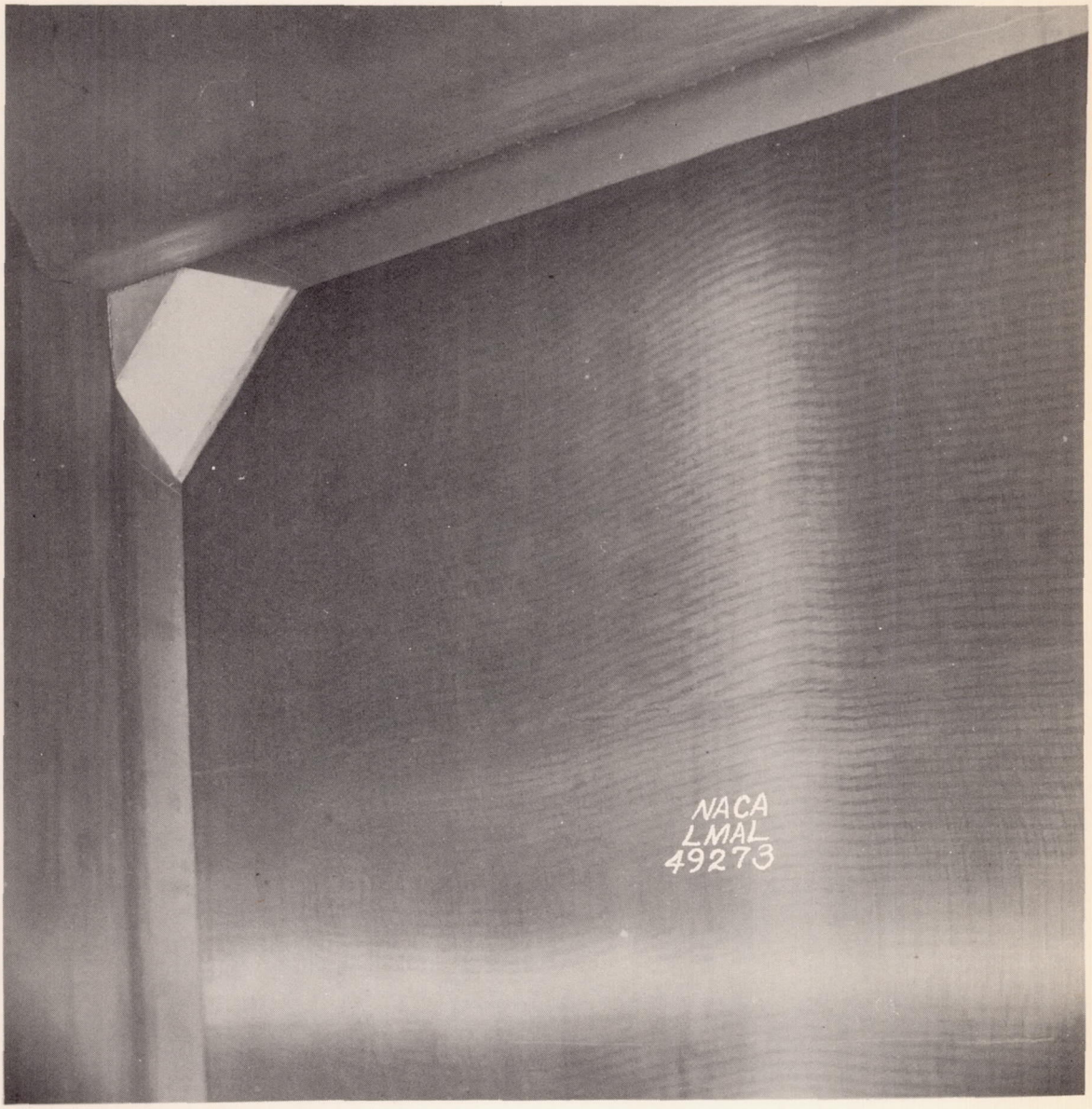

Figure 11.- Turbulence-reducing screen installation in the Langley two-dimensional low-turbulence pressure tunnel, looking upstream toward upper left-hand corner.

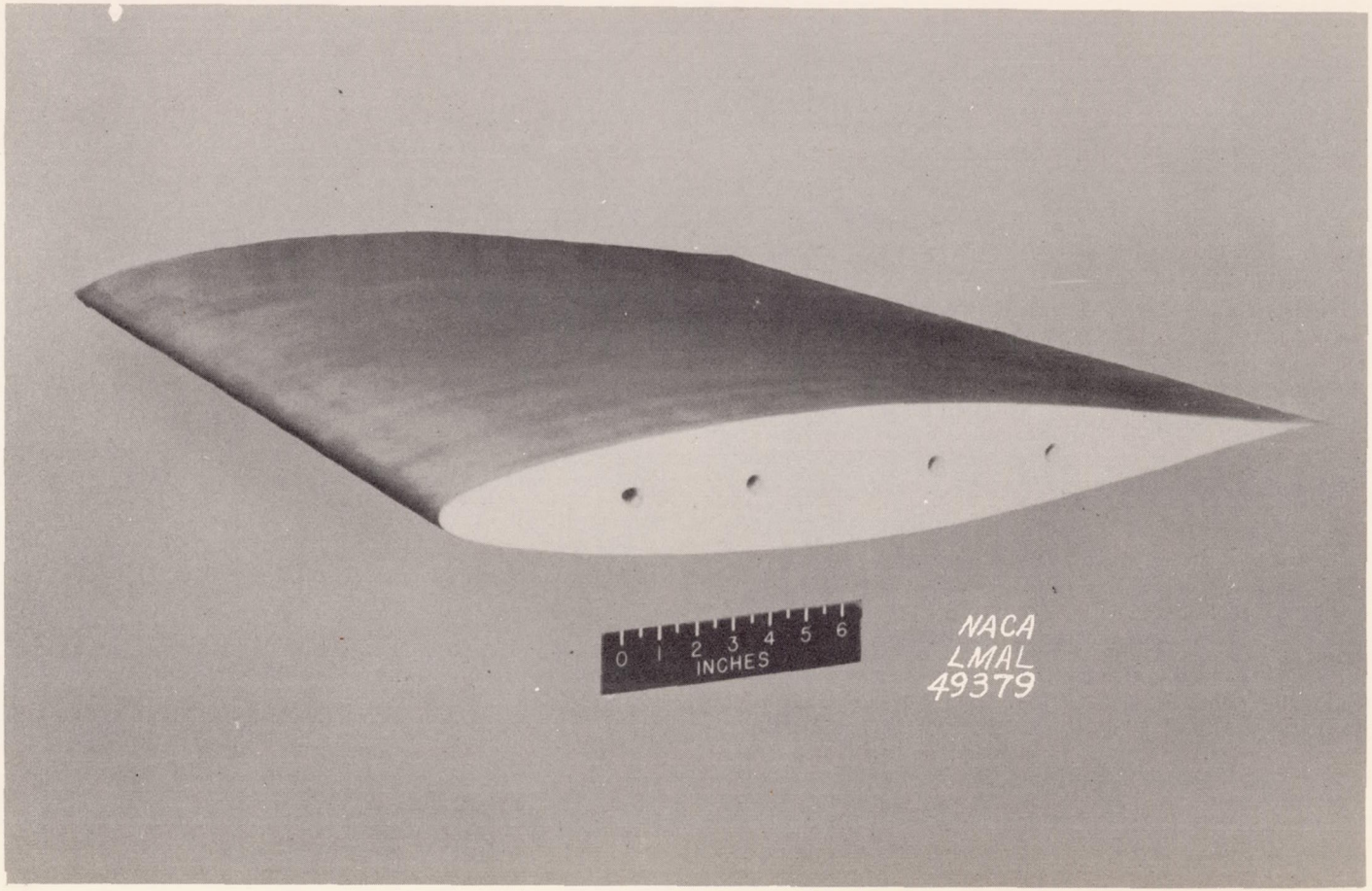

Figure 12.- Typical 24-inch-chord airfoil-section model tested in the Langley two-dimensional low-turbulence pressure tunnel.

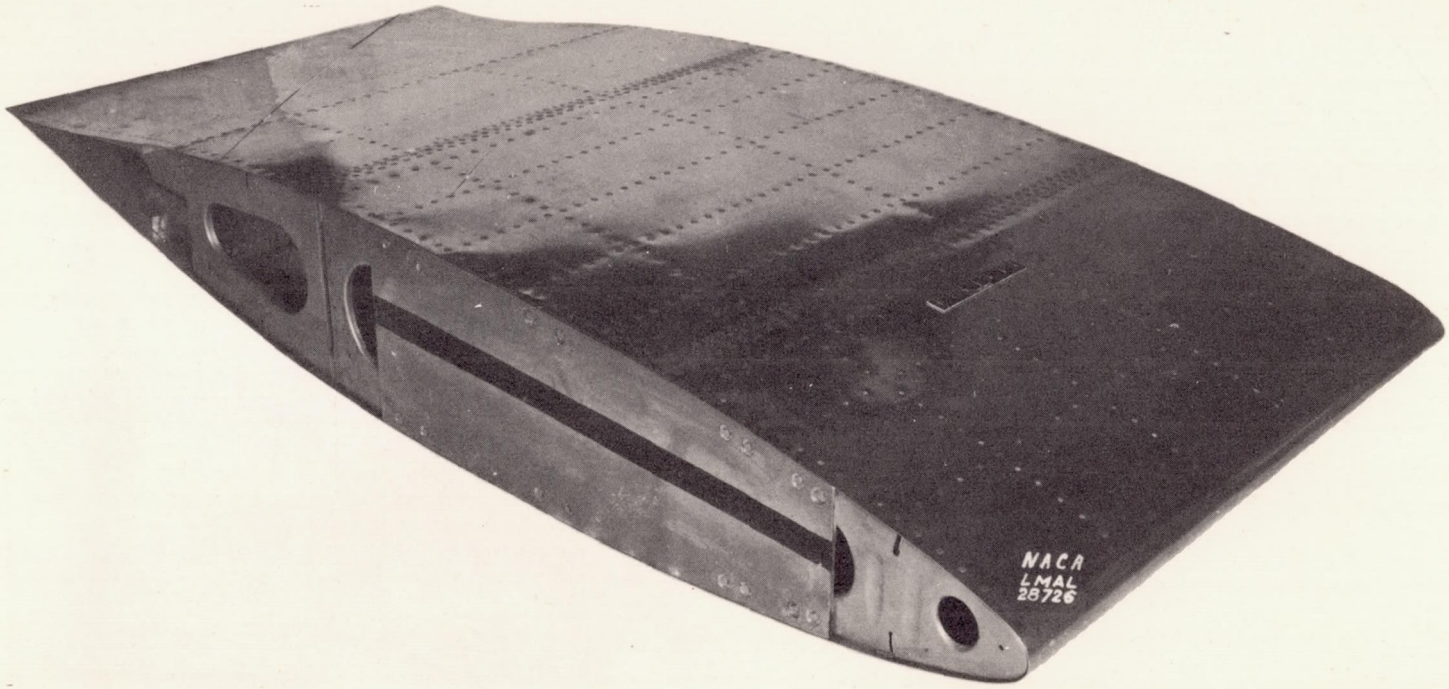

Figure 13.- Large-chord practical-construction wing section, without surface finishing, tested in the Langley two-dimensional low-turbulence pressure tunnel.

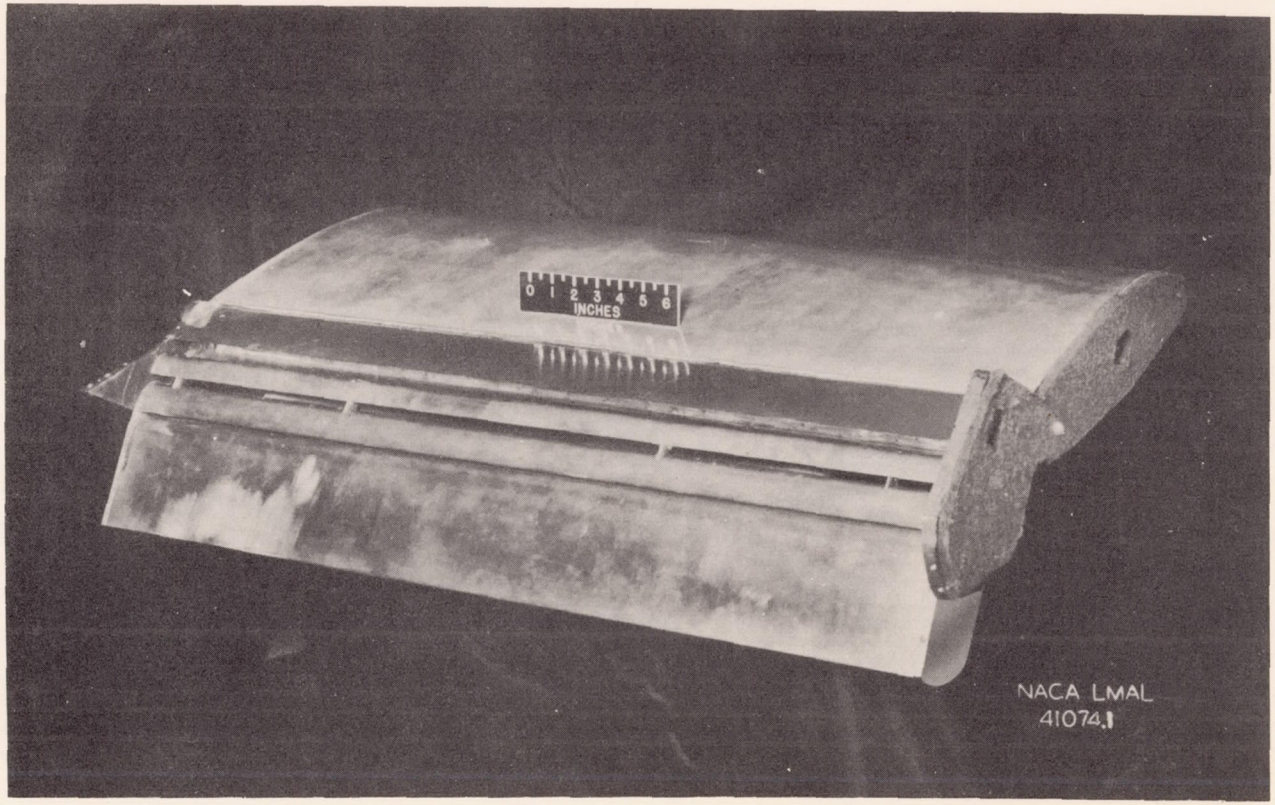

(a) Model with lateral-control and high-lift devices.

Figure 14.- Typical models tested in the Langley two-dimensional low-turbulence tunnels.

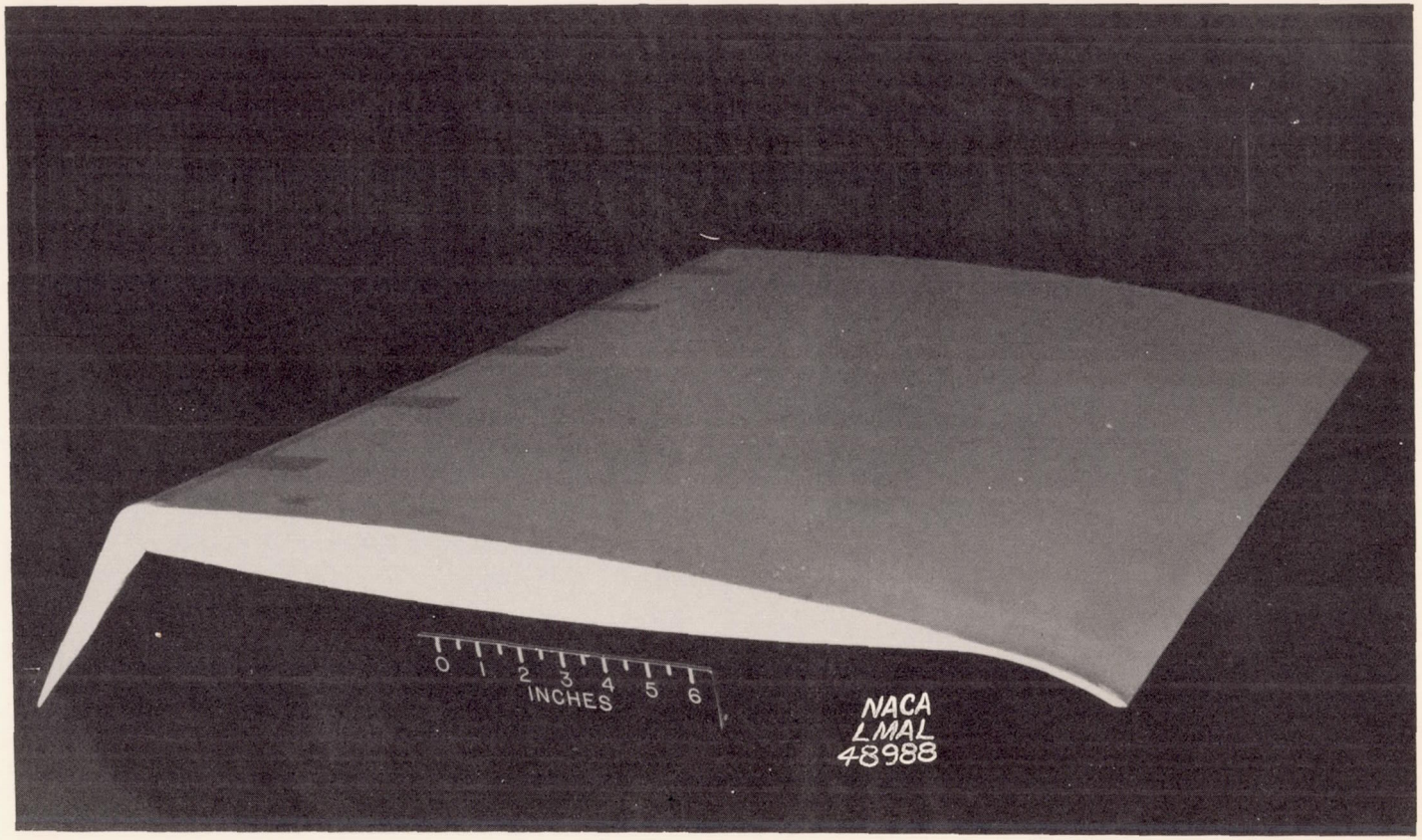

(b) Circular-arc airfoil-section model with leading- and trailing-edge flaps.

Figure 14.- Concluded.

Figure 15.- Model with leading-edge air intake tested in the Langley two-dimensional low-turbulence tunnels.

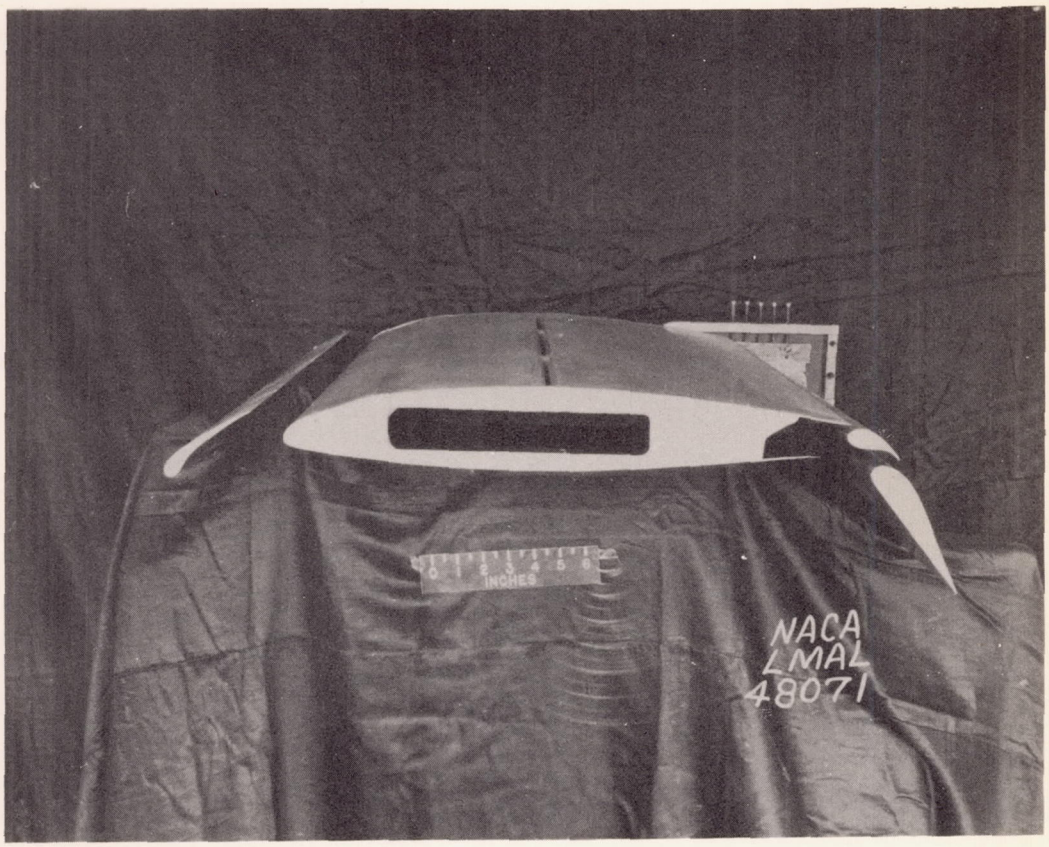

Figure 16.- Model with boundary-layer suction slot, leading-edge slat, and double-slotted trailing-edge flap tested in the Langley two-dimensional low-turbulence tunnels.

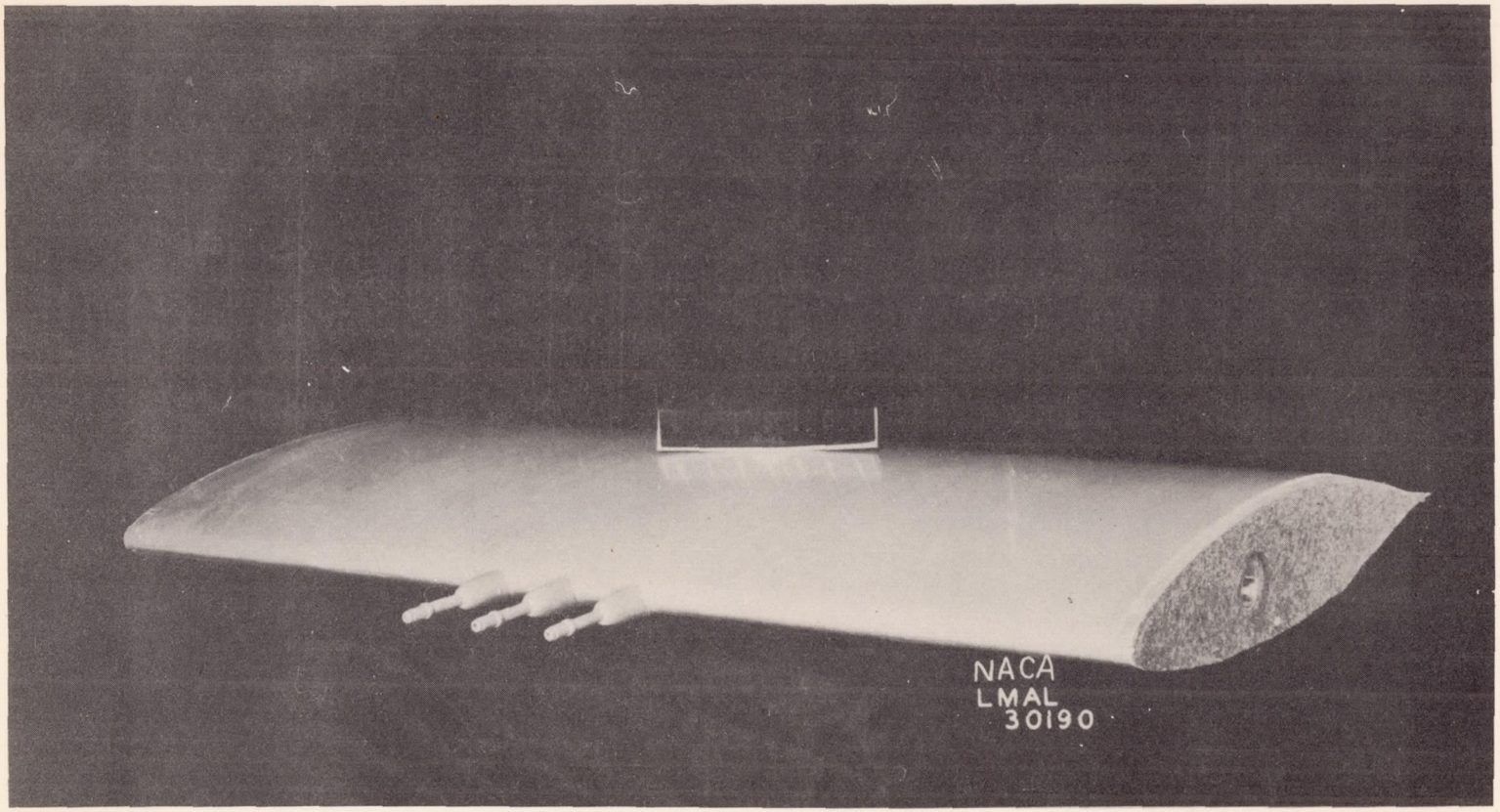

(a) Model with simulated 20-millimeter cannons installed in the nose.

Figure 17.- Models tested in the Langley two-dimensional low-turbulence pressure tunnel to study interference effects of wing-body combinations.

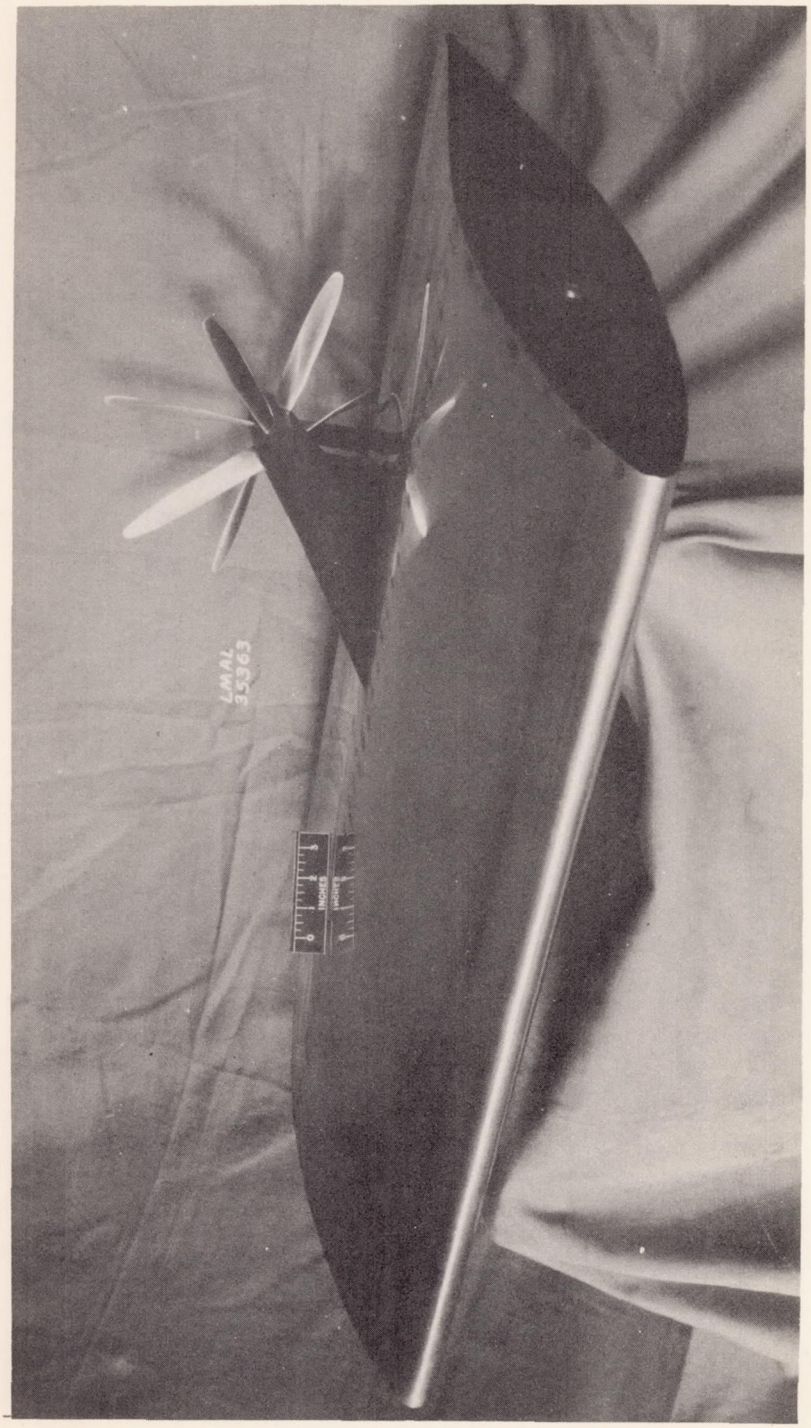

(b) Model with pusher-propeller installation.

Figure 17.- Concluded.

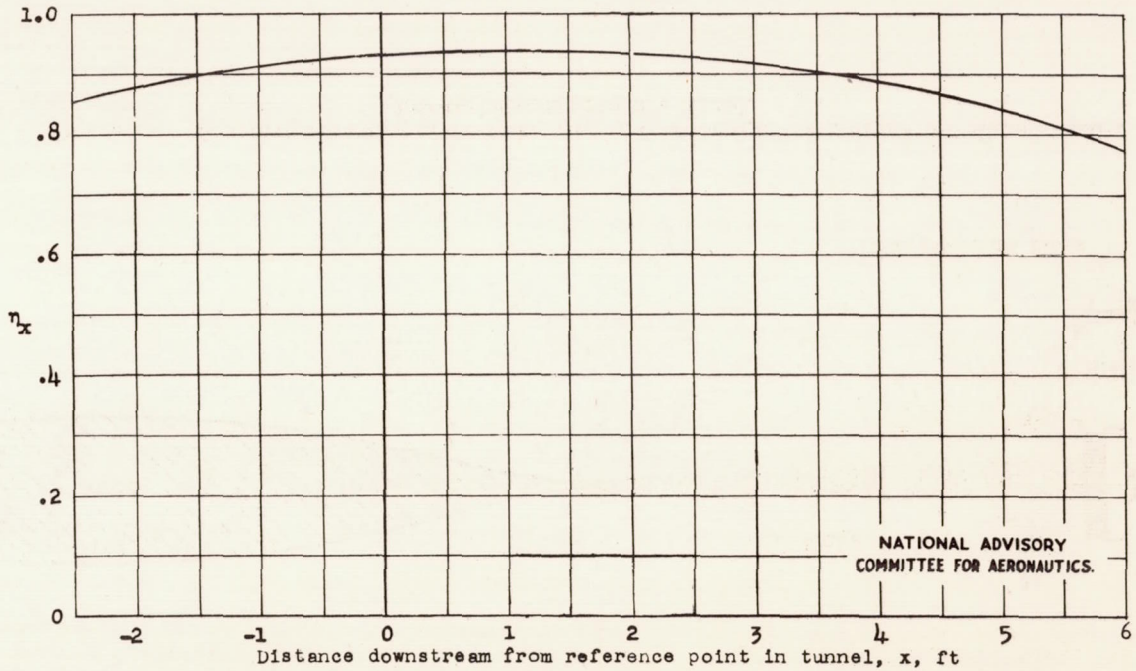

Figure 18.- Lift efficiency factor η_x for a point vortex situated at various positions along the center line of the tunnel.

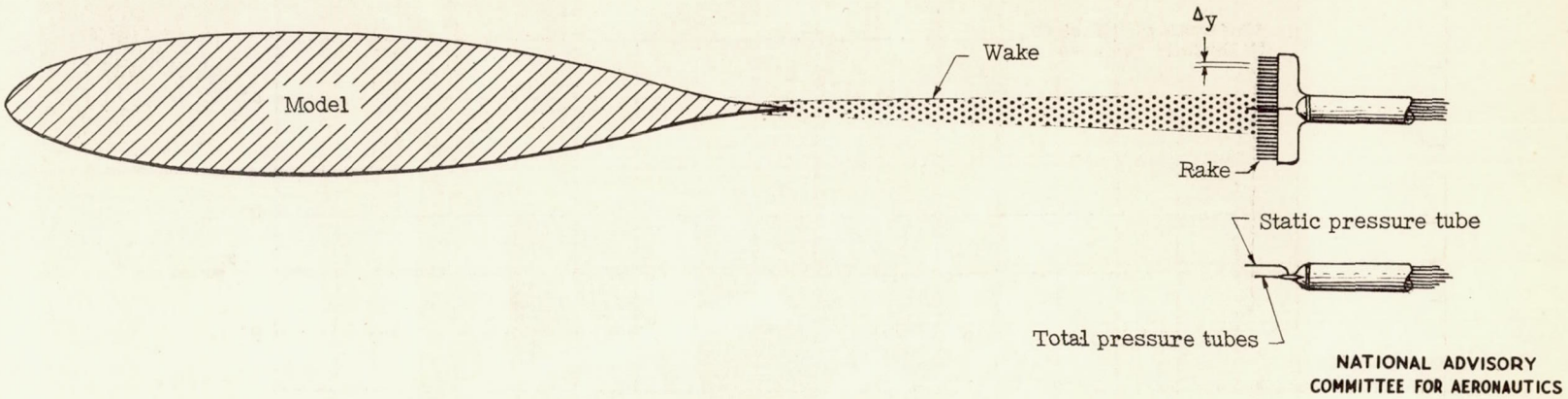

Figure 19.- Schematic drawing of the wake-survey rake used in the Langley two-dimensional low-turbulence pressure tunnel.

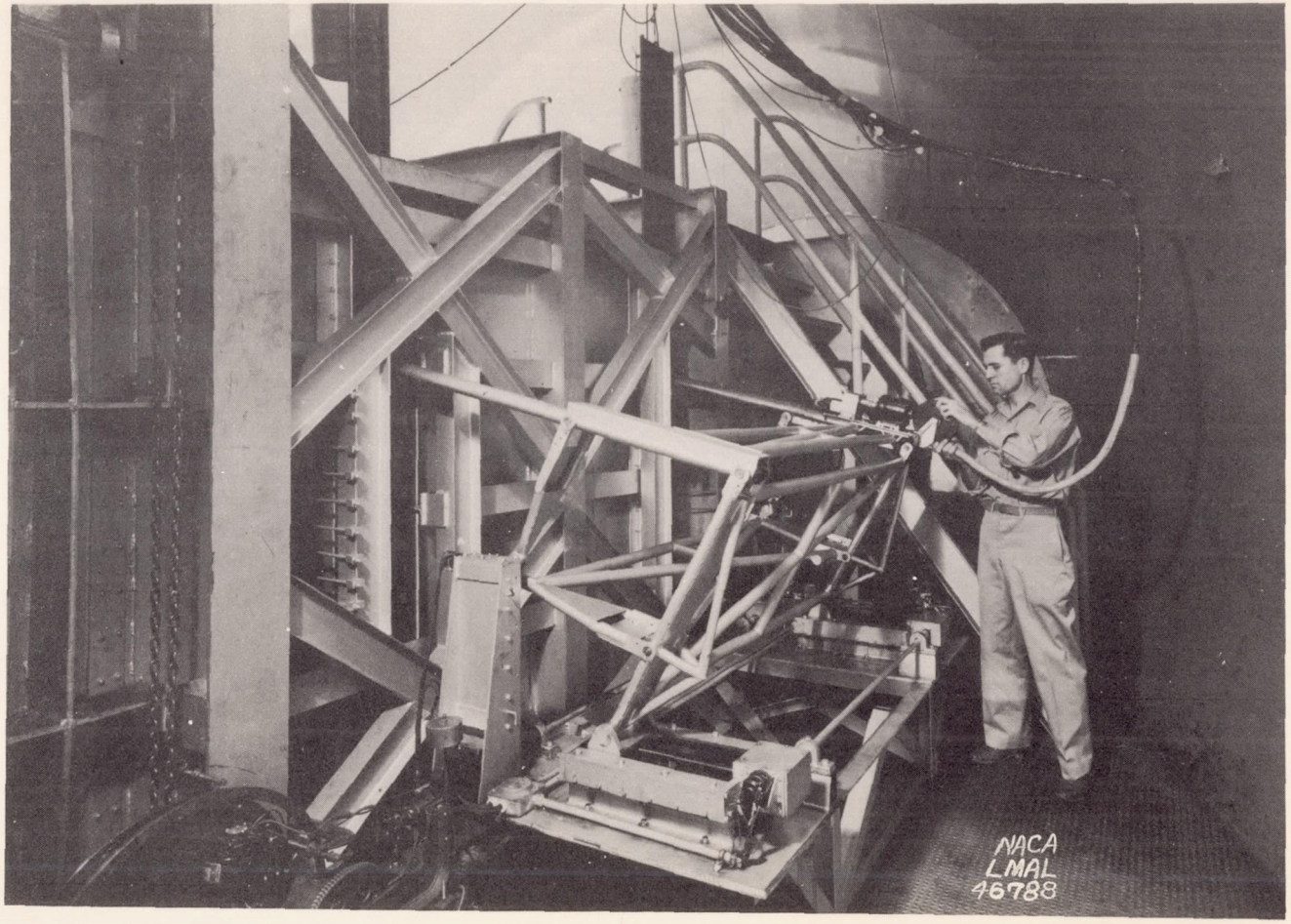

Figure 20.- Wake-survey-apparatus mechanism used in the Langley two-dimensional low-turbulence pressure tunnel.

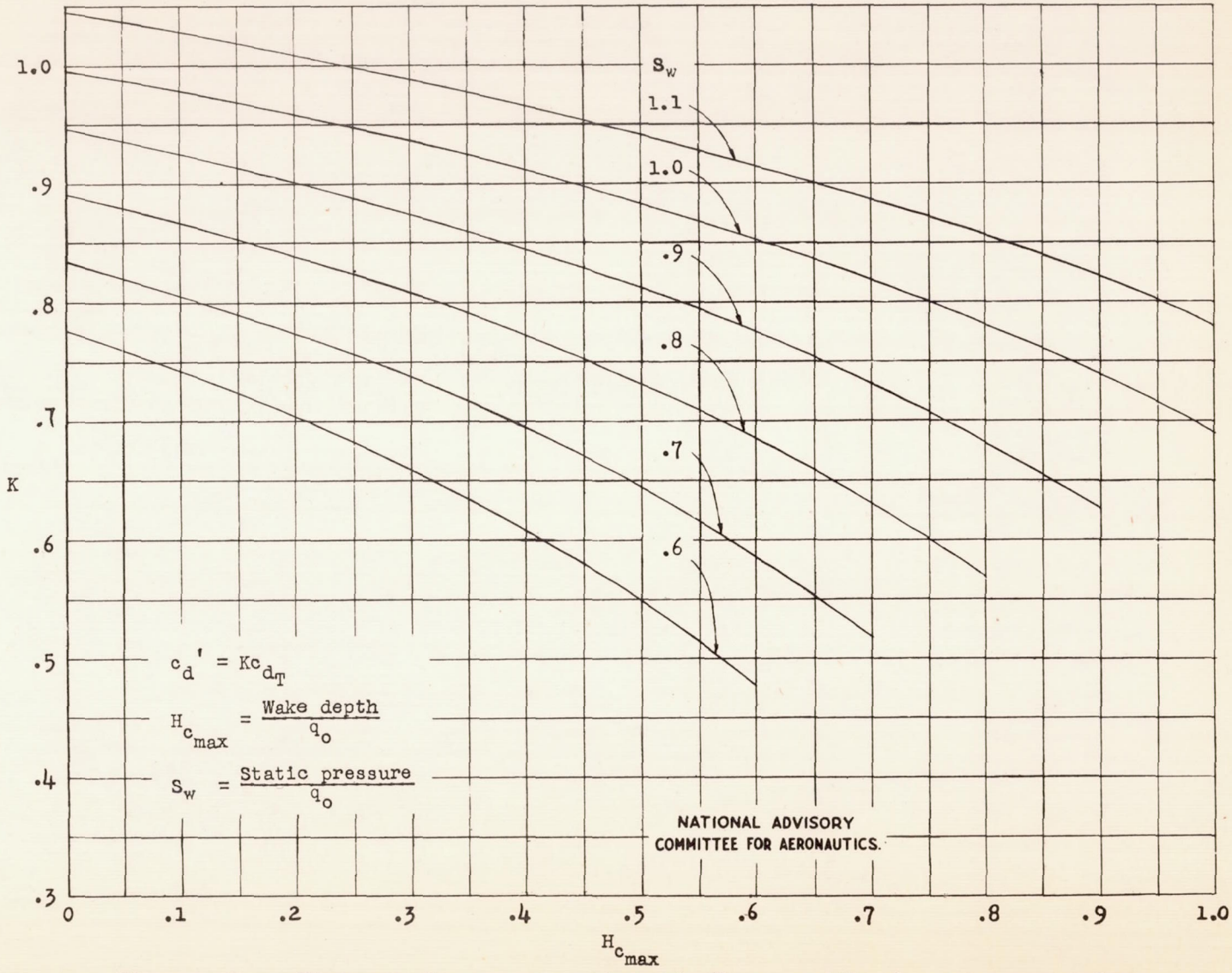

Figure 21.- Plot of K as a function of $H_{c_{max}}$ with S_w as a parameter.

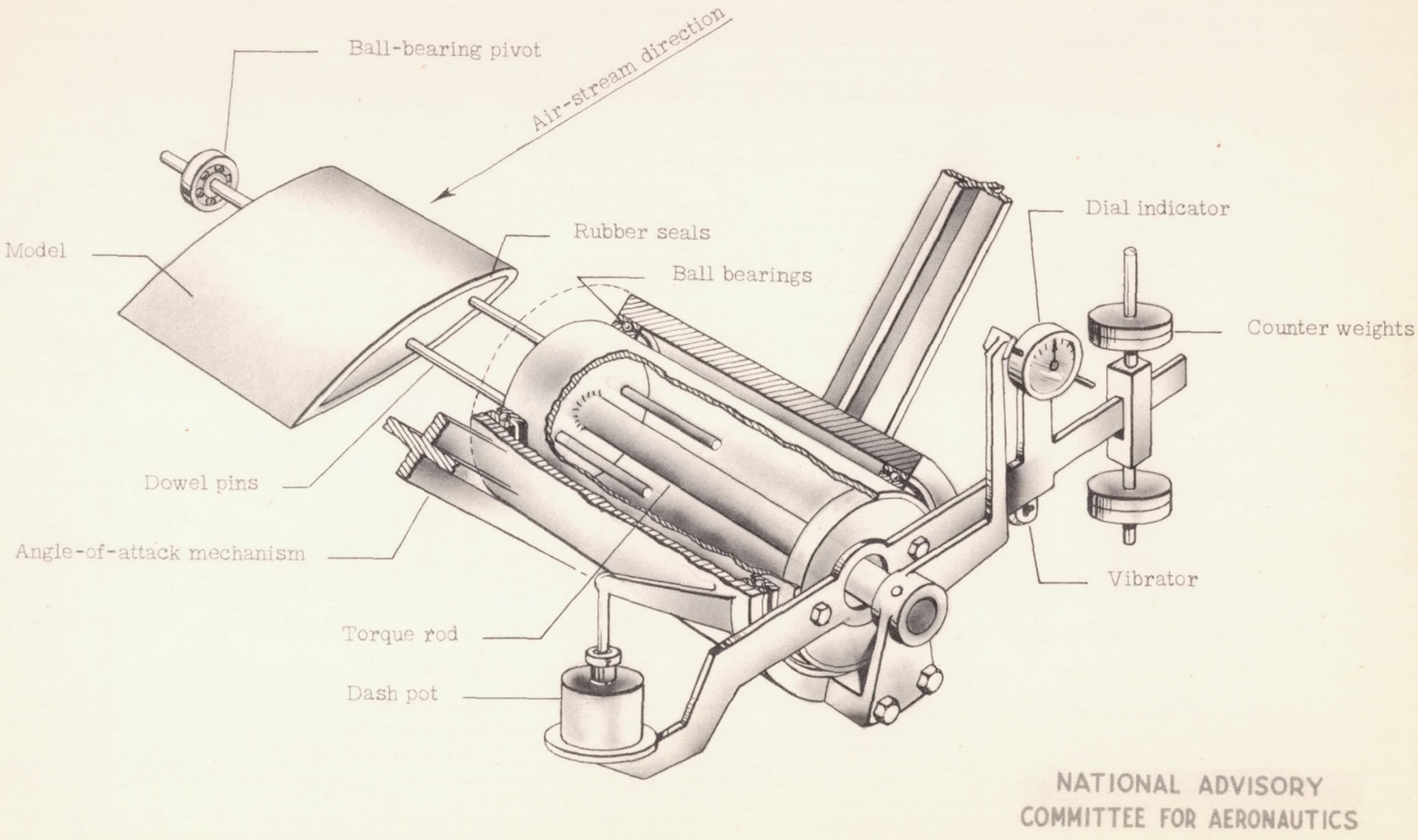

Figure 22.- Torque-rod moment balance installed in the Langley two-dimensional low-turbulence pressure tunnel.

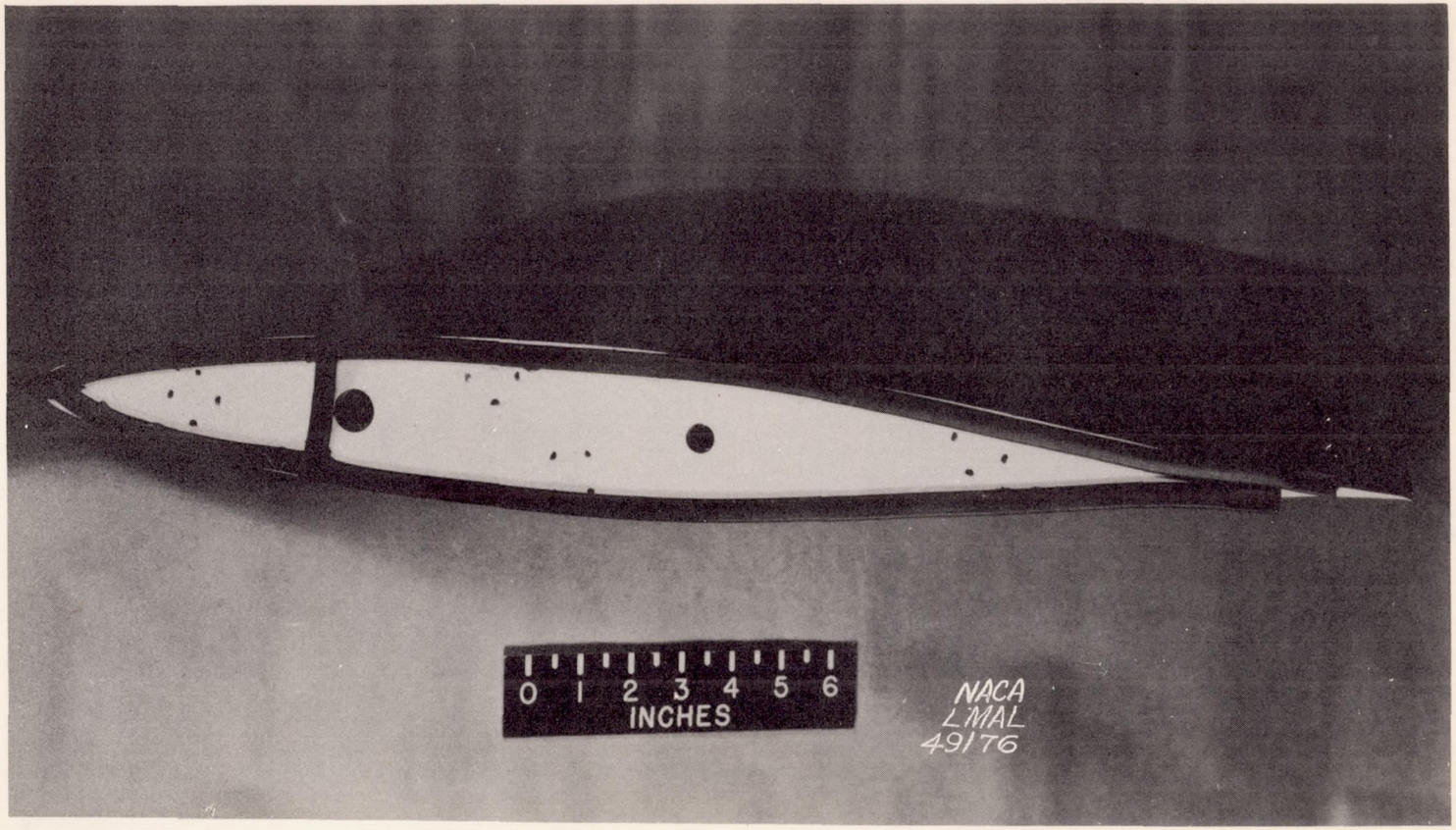

Figure 23.- Rubber seals attached to ends of model for pitching-moment test in the Langley two-dimensional low-turbulence pressure tunnel.

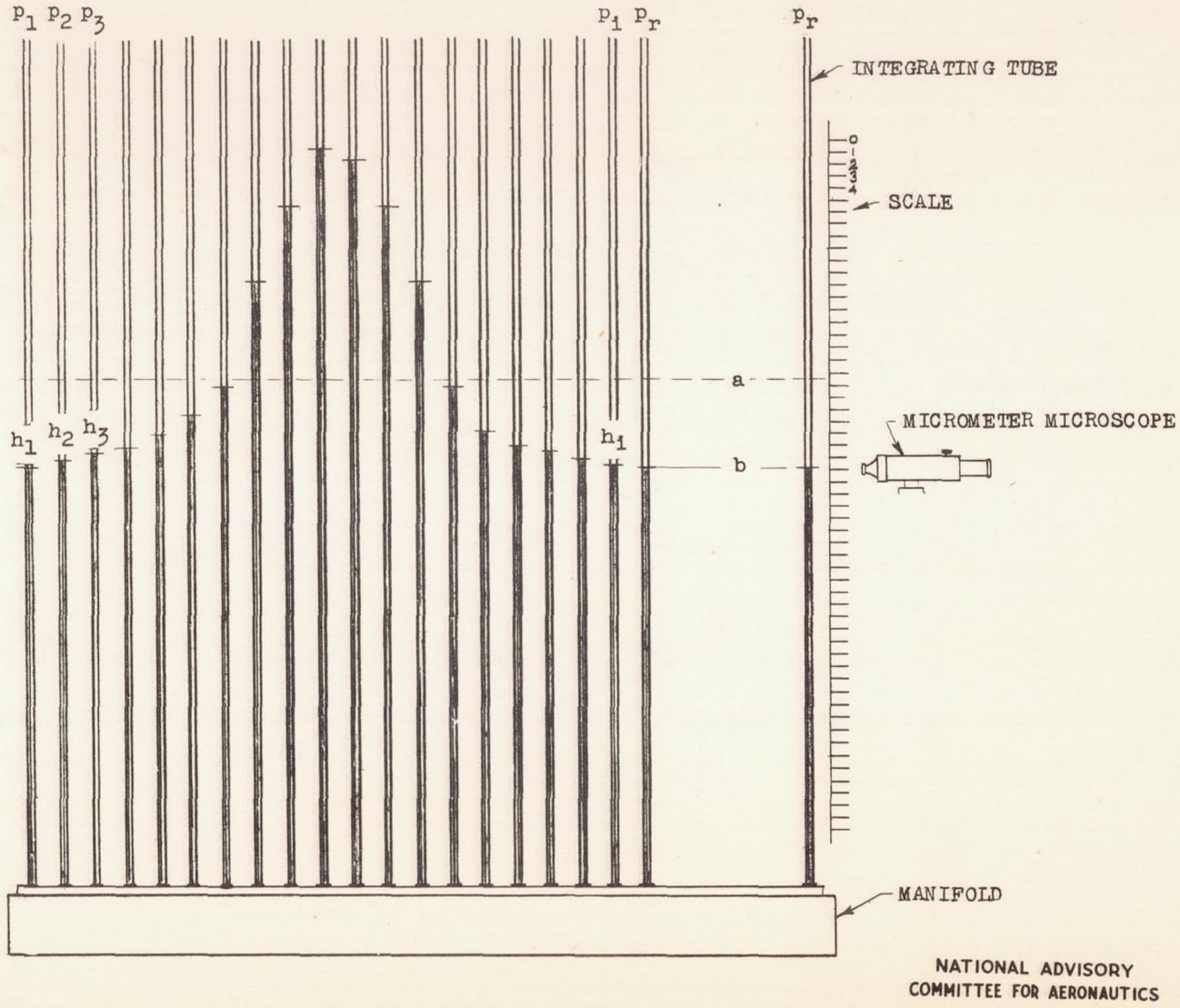

Figure 24 .- Schematic drawing of an integrating manometer.

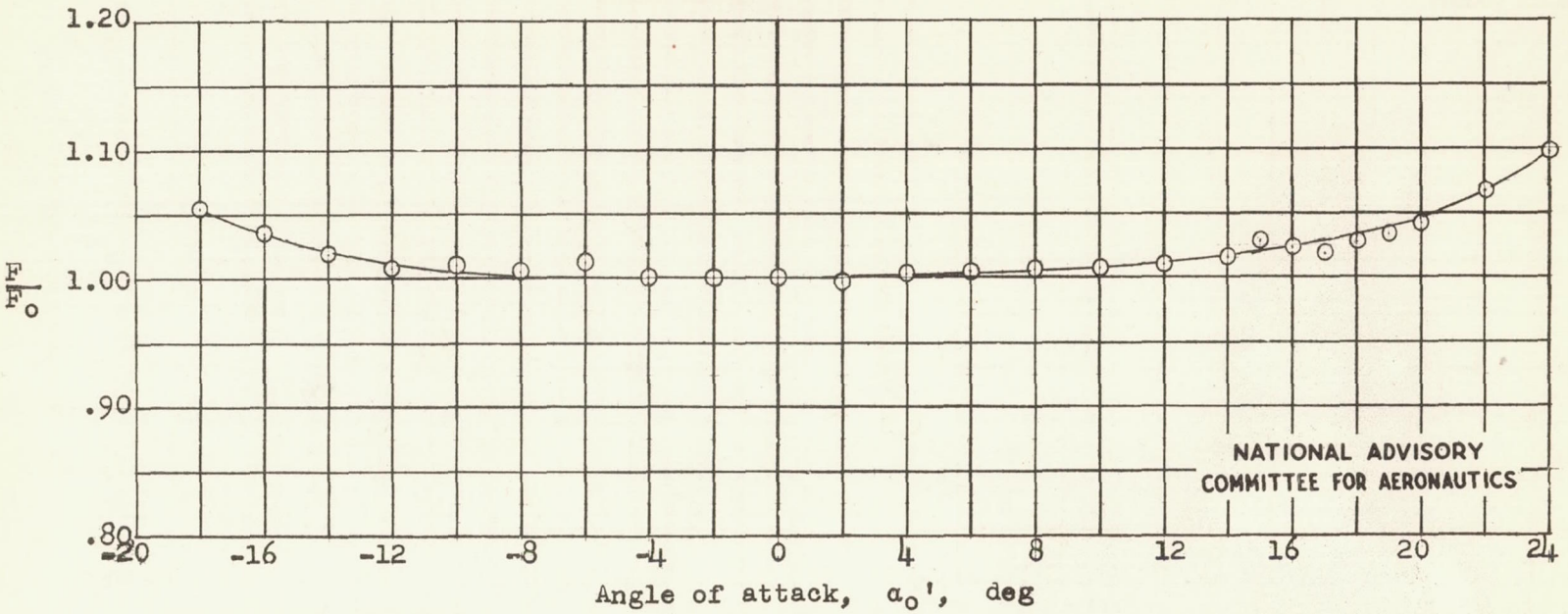

Figure 25.- Additional blocking factor at the tunnel walls plotted against angle of attack for the NACA 64_3-418 airfoil.

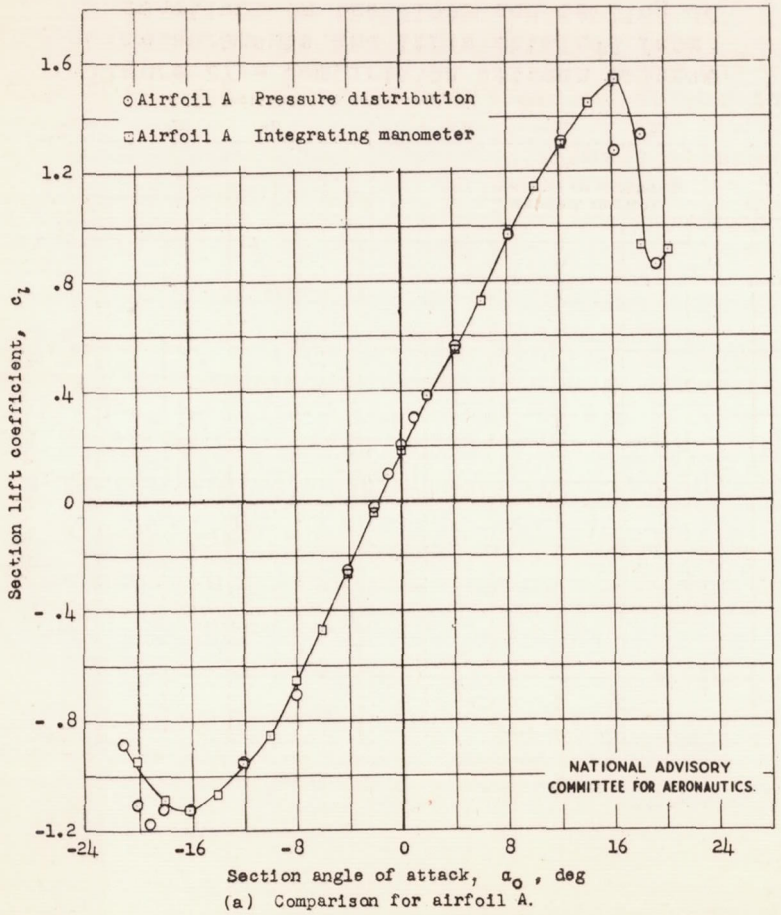

(a) Comparison for airfoil A.

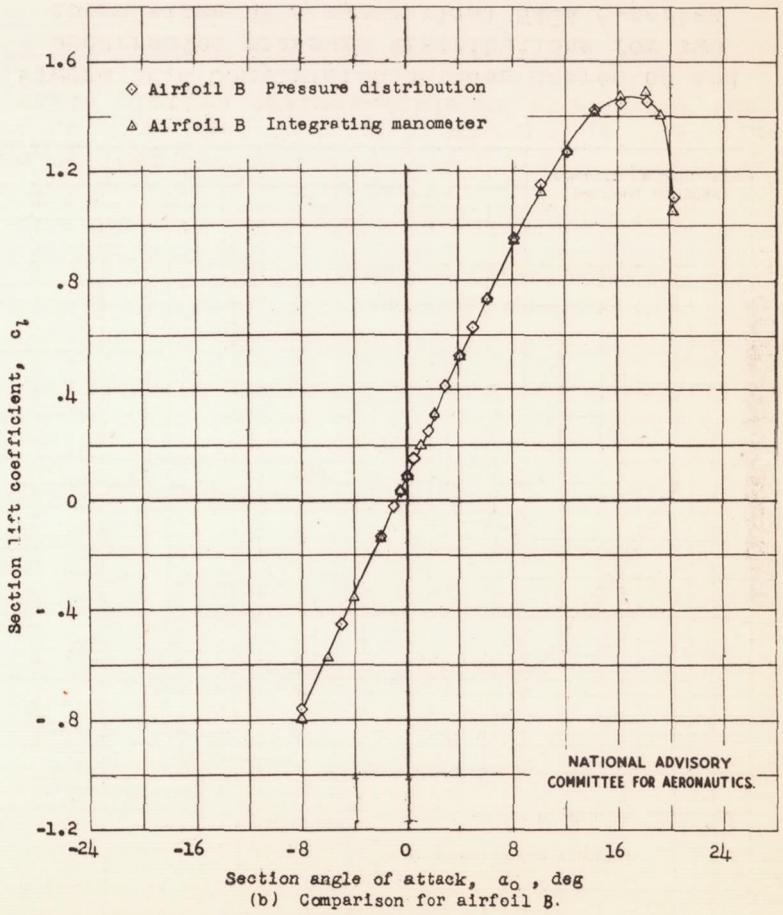

(b) Comparison for airfoil B.

Figure 26.- Comparison between lifts obtained from pressure-distribution measurements and lifts obtained from reactions on the floor and ceiling of the tunnel.

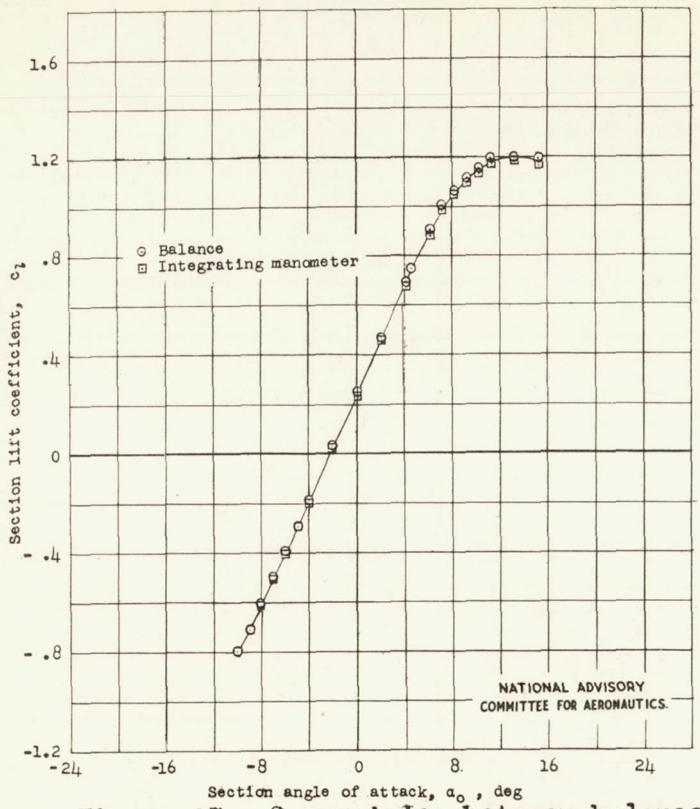

Figure 27.- Comparision between balance measurements and lifts obtained from reactions on the floor and ceiling of the tunnel.

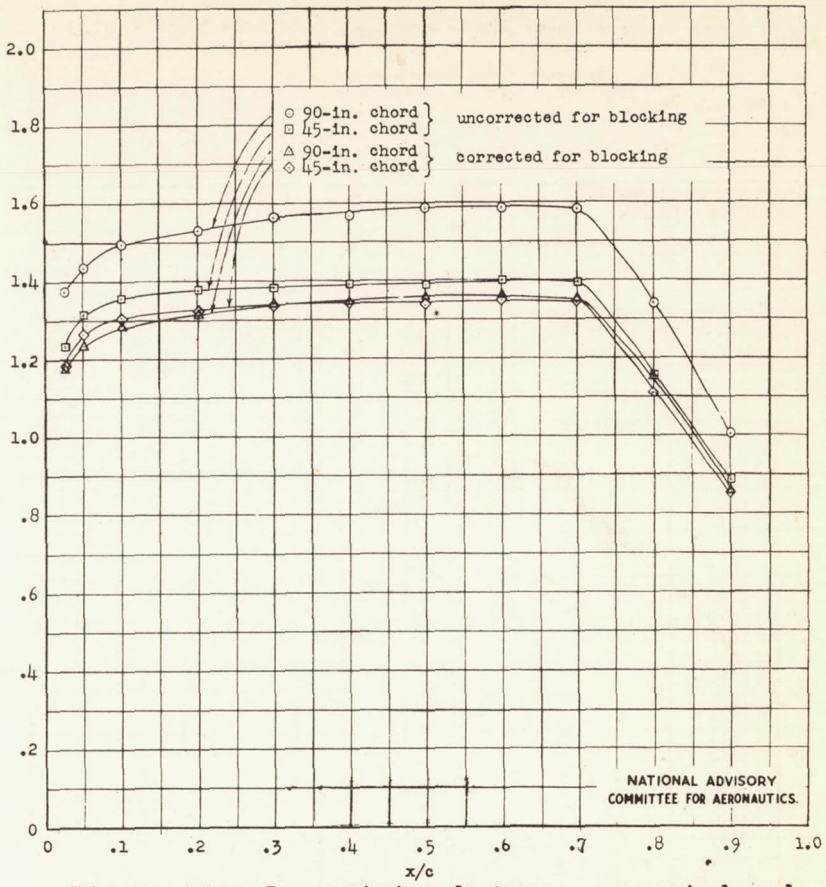

Figure 28.- Comparision between corrected and uncorrected pressure distributions for two chord sizes of a symmetrical NACA 6-series airfoil of 15-percent thickness. $\alpha_o = 0°$.

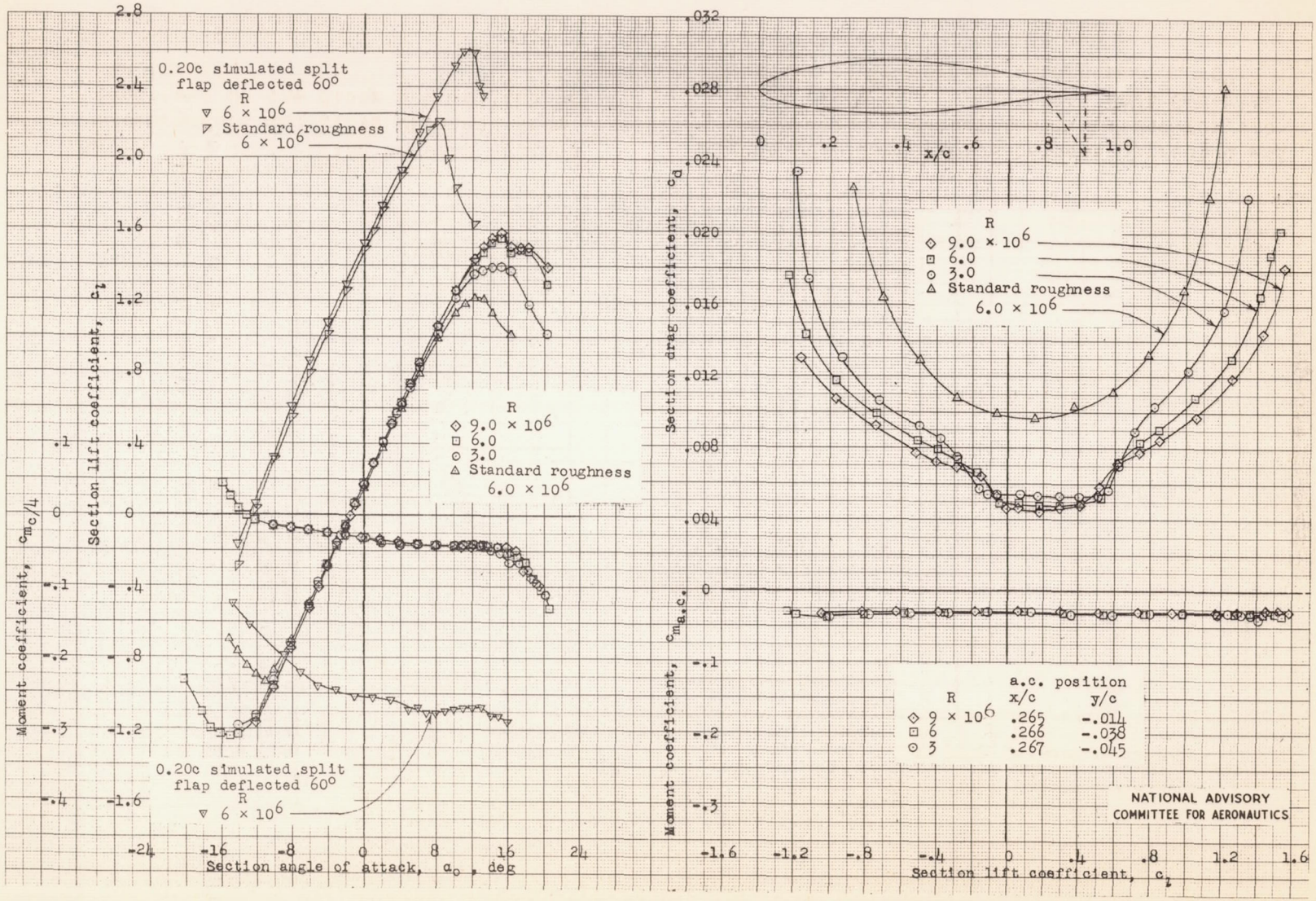

Figure 29.- Aerodynamic characteristics of NACA 64_2-215 airfoil section of 24-inch chord tested in the Langley two-dimensional low-turbulence pressure tunnel.

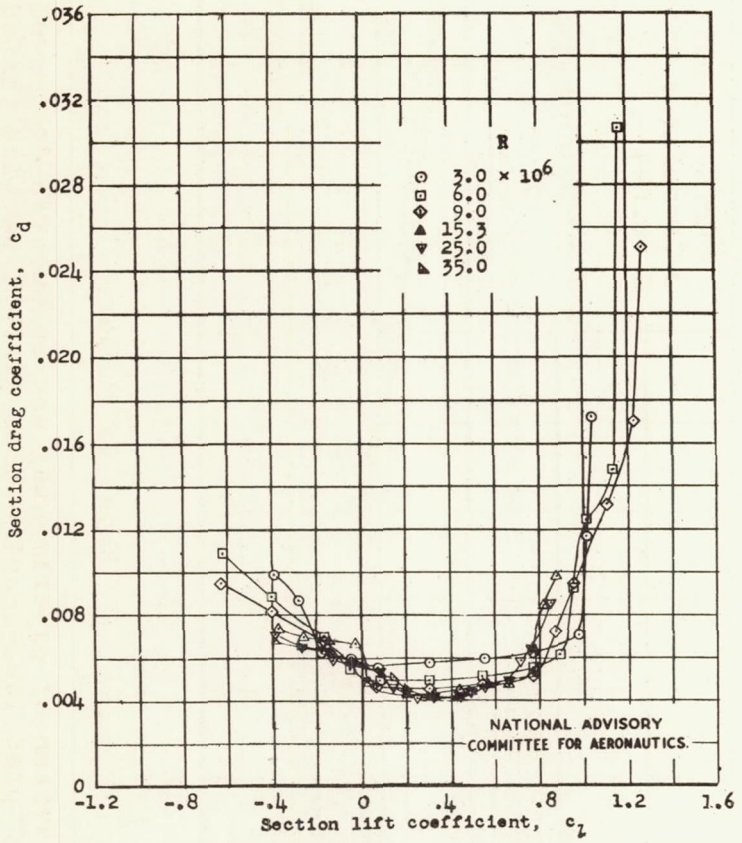

Figure 30.- Variation of low-drag range with Reynolds number for the NACA $65_{(421)}$-420 airfoil.

NATIONAL ADVISORY
COMMITTEE FOR AERONAUTICS

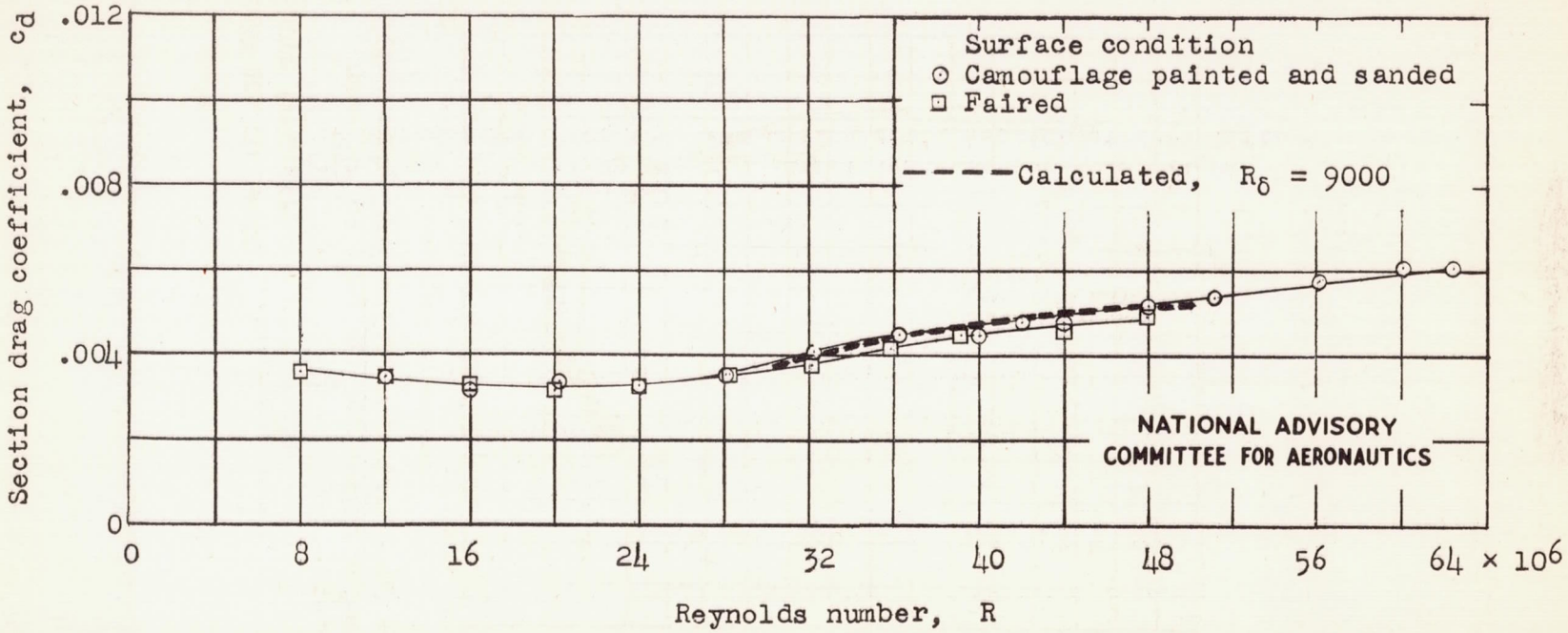

Figure 31.- Comparison of experimental and calculated drag-scale-effect curves for large-chord practical-construction airfoil section tested in the Langley two-dimensional low-turbulence pressure tunnel.

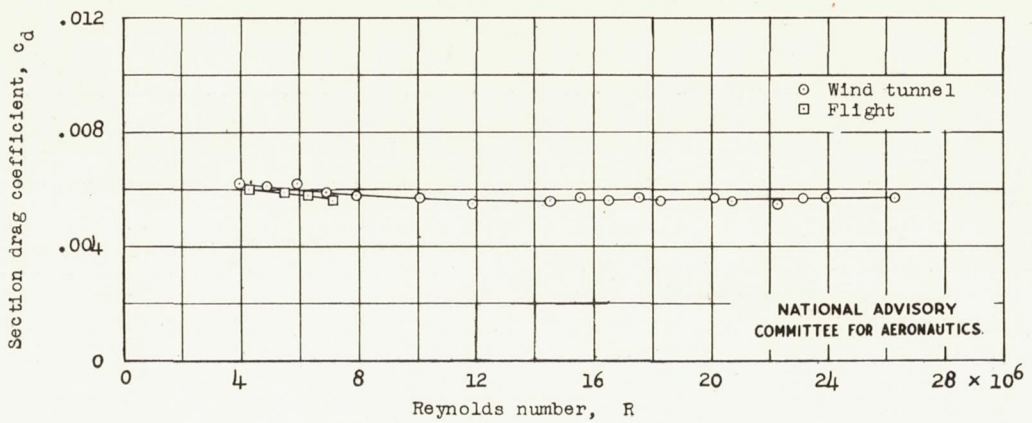

Figure 32.- Comparison of drag coefficients measured in flight and wind tunnel for the NACA 0012 airfoil section at zero lift.